Tetrahedron: *Asymmetry* 24 (2013) 89–103

Contents lists available at SciVerse ScienceDirect

Tetrahedron: *Asymmetry*

journal homepage: www.elsevier.com/locate/tetasy

Thermal and $Sc(OTf)_3$ catalyzed 1,3-dipolar cycloaddition of open-chain nitrones to α,β-unsaturated lactones: combined experimental and computational studies

Marcin Śnieżek, Sebastian Stecko *, Irma Panfil, Bartłomiej Furman, Zofia Urbańczyk-Lipkowska, Marek Chmielewski

Institute of Organic Chemistry, Polish Academy of Sciences, Kasprzaka 44/52, 01-224 Warsaw, Poland

ARTICLE INFO

Article history:
Received 25 October 2012
Accepted 14 December 2012

ABSTRACT

The stereoselectivity of 1,3-dipolar cycloaddition reactions of *C*-phenyl open-chain nitrones and α,β-unsaturated γ- and δ-lactones was investigated under thermal and catalytic conditions. It was found that under thermal conditions, the *endo* approach of the reactants was preferred leading to the thermodynamic product. In the presence of $Sc(OTf)_3$ the *exo* adduct was obtained in high yield and selectivity. The energies of the cycloaddition reactions were investigated by means of molecular orbital calculations at the B3LYP/6-31+G(d,p) and MP3/6-31+G(d,p) theory level. Different reaction channels and reactant approaches, fitting the individual regio- and stereochemical preferences, are discussed. The computational results were compared with the corresponding experimental data and found to be in good agreement.

1. Introduction

Since discovery of penicillin, β-lactam antibiotics represent one of the most powerful tools against bacterial infections. Over the last 25 years, they have also been found to exhibit a variety of interesting activities against some non-bacterial diseases.[1]

In 1979 Tufariello et al.[2] reported a simple and attractive entry to the basic skeleton of thienamycin based on the 1,3-dipolar

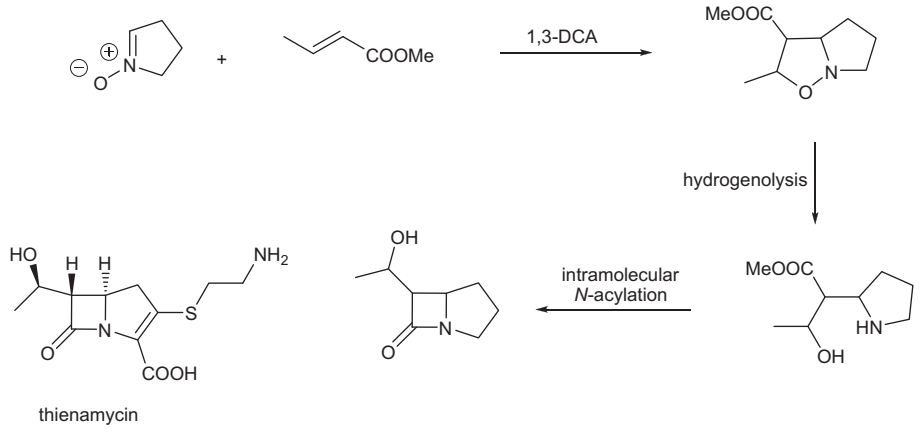

Scheme 1.

* Corresponding author. Tel.: +48 22 343 2137; fax: +48 22 632 6681.
E-mail address: sebastian.stecko@icho.edu.pl (S. Stecko).

0957-4166/$ - see front matter © 2012 Elsevier Ltd. All rights reserved.
http://dx.doi.org/10.1016/j.tetasy.2012.12.006

cycloaddition (1,3-DCA) of a five-membered cyclic nitrone and methyl crotonate. The general strategy of synthesis, which was such as **1**–**8**, however, one prerequisite must be fulfilled, the key cycloaddition step must proceed with high stereoselectivity.

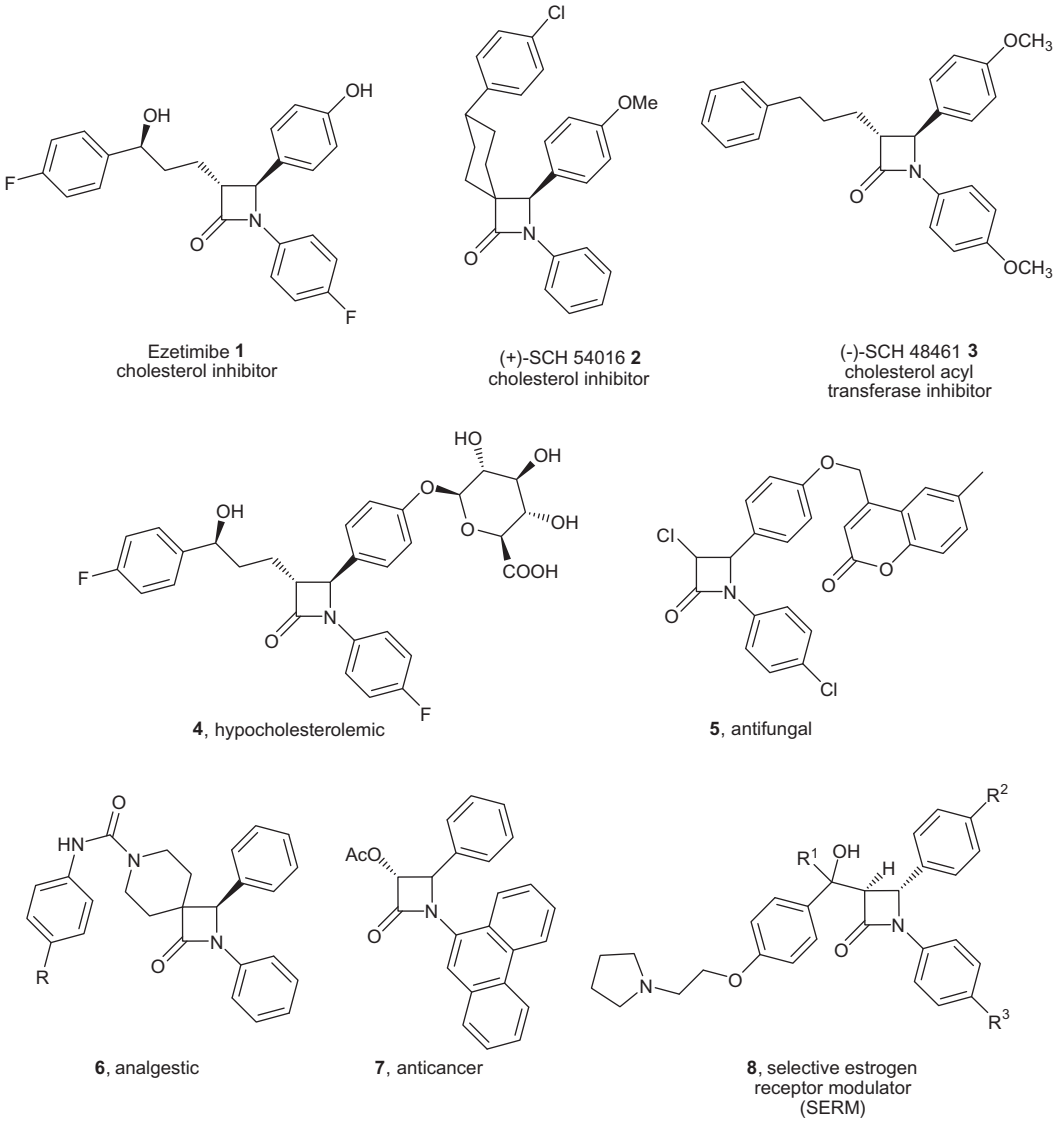

based on the formation of an isoxazolidine adduct, followed by hydrogenolysis of the *N*,*O*-bond to give a β-amino acid and its subsequent cyclization leading to the β-lactam ring (Scheme 1), has been exploited in a variety of target oriented syntheses[3].

Tufariello's strategy also offers a particularly attractive entry to *N*,4-diaryl substituted β-lactams. Compounds, which belong to this group, for instance **1**–**8**, exhibit a wide range of interesting biological activities such as cholesterol absorption inhibition (compounds **1**–**4**),[4] antifungal (compound **5**),[5] and analgesic activity (compound **6**)[6] or anticancer properties (compounds **7**–**8**).[7]

It is important to note that the biological properties of β-lactam compounds **1**–**8** are directly related to the configuration of the stereogenic centers in the 2-azetidinone ring. The presence of *trans*- or *cis*-substitution pattern at the ring is important for the bioactivity of these compounds.

As mentioned, the Tufariello strategy is a useful tool for the synthesis of the central structural fragment of bioactive monobactams

Previously we had demonstrated that cyclic dipolarophiles, such as sugar-derived δ-lactone **9**, are attractive reagents for the thermally induced 1,3-DCA furnishing adducts, which in turn can be transformed into the corresponding 2-azetidinones. For example, the adduct of lactone **9** with *C*-anisyl-*N*-phenyl nitrone **10** was converted into 1,4-diaryl β-lactam **11** with a polyol side chain at the C-3 carbon atom.[8]

Independently, we have demonstrated the stereocontrolled transformation of adducts of simple five-membered cyclic nitrones (e.g. **17** and its chiral substituted derivatives) and γ- and δ-lactones **12**, **14**, and **15** into selected iminosugars.[9] These syntheses[9,10] prompted us to investigate, in greater detail, factors responsible for the stereoselectivity of the 1,3-dipolar cycloaddition process. Our experimental studies were combined with quantum mechanic computations, studying in detail the reaction mechanism, its *exo*/*endo*- and facial selectivity,[11] as well as the chiraloopical properties of the cycloadducts.[12]

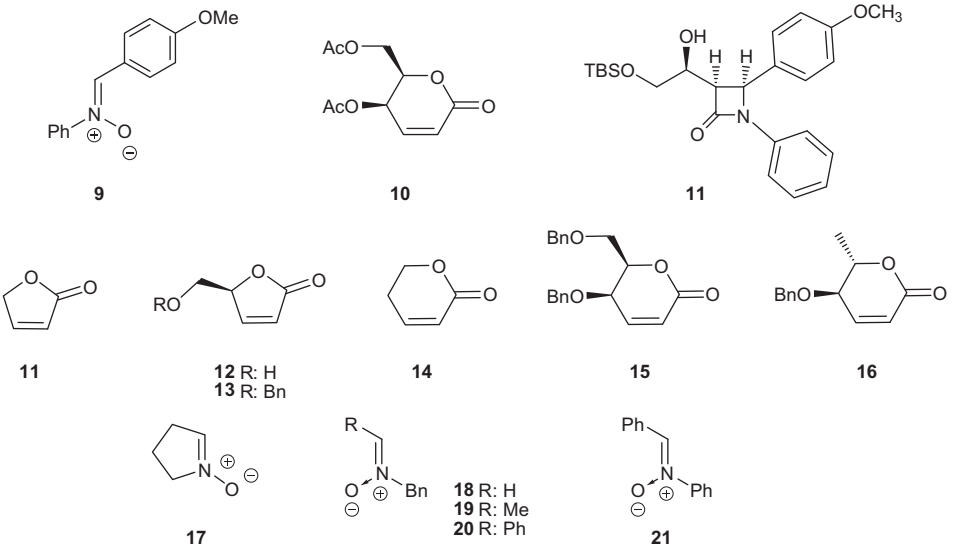

We have recently reported on the application of diaryl nitrones in a formal synthesis of Ezetimibe **1**,[13] and related compounds[14] via Cu(I)-mediated Kinugasa cycloaddition/rearrangement cascade reactions between terminal acetylenes[15] derived from L-glyceraldehyde acetonide and suitable *C*,*N*-diarylnitrones.

Finally, bearing in mind that the 4-aryl and *N*,4-diaryl azetidinones exhibit particularly interesting biological properties,[4–7] we have revisited our previous work on the cycloaddition reactions of nitrones, but focused our attention on 1,3-dipolar cycloadditions involving diaryl nitrone **21** with α,β-unsaturated γ- and δ-lactones **11**–**16**. Herein our aim was to find a way to achieve stereochemical control of the configuration of the newly formed stereogenic centers. We focused our attention on the *exo*/*endo* selectivity as a function of the reaction time, as well as the thermal and catalytic conditions of the cycloaddition reaction.

2. Results and discussion

2.1. Thermal 1,3-dipolar cycloaddition of nitrones to unsaturated lactones

Herein we selected lactones **11**–**16** and the nitrones **18**–**21**. All sugar-derived lactones were obtained following known methods.[16] The nitrones were synthesized using common methods by reacting the corresponding aldehydes with phenyl- or benzylhydroxylamine.[17] Thermal cycloaddition reactions were performed following standard procedures,[8] by reacting the nitrone and dipolarophile in toluene solution at reflux; at room temperature, the formation of products was not observed, even after extension of the reaction time for up to 1 week.

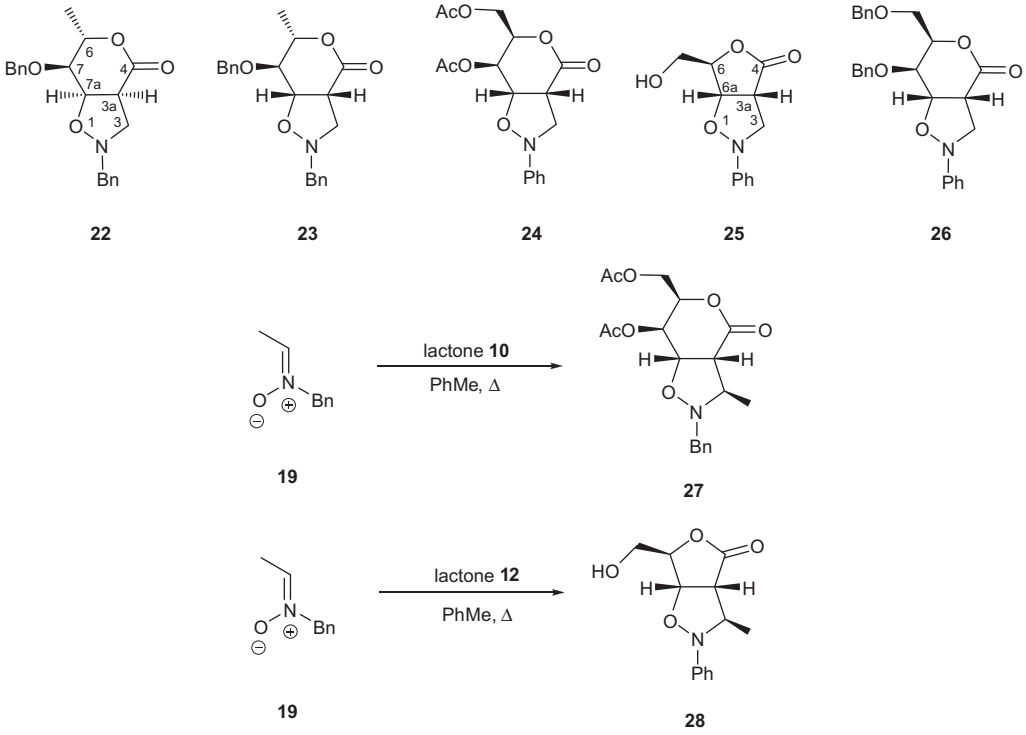

Scheme 2.

In the case of L-*erythro* lactones, such as **16**, due to the *anti* substitution of a six-membered ring, even the simple nitrone **18** provided a mixture of adducts **22** and **23** in a ratio of approximately 2.5:1, respectively, as a result of the addition to both sides of the lactone ring (Scheme 5).[18] These reactions, therefore, were not investigated further since their usefulness in context of our goal, that is, target-oriented syntheses, appeared to be limited. In other cases explored, the nitrone molecule approached the double bond exclusively *anti* to the substituent or both substituents in the lactone (**10**, **12**, and **15**). Thus, the simple nitrone **18** with lactones **10**, **12**, and **15** gave adducts **24**, **25**, and **26**, respectively (Scheme 2).[8]

Due to the disfavored interaction of the methyl group with the lactone carbonyl group, *N*-benzyl-*C*-methyl nitrone **19** approaches lactones **10** and **12** in the *endo* mode to provide the corresponding adducts **27** and **28** (56%), which are the thermodynamic products; in these cases the formation of the corresponding *exo* isomers was not observed (Scheme 2).[8]

From a synthetic point of view, the *C*,*N*-disubsitituted nitrones **20** and **21** represent suitable substrates for the synthesis of bioactive *N*,4-diaryl-2-azetidinones. However, our previous studies showed that the reaction of nitrones **20** and **21** with lactones **10**–**15** furnish, under thermal conditions, the corresponding mixtures of *exo* and *endo* adducts. Moreover, the ratio of the resulting adducts is difficult to predict, while at the same time the ratio plays a critical role in controlling the configuration at C-4 of the azetidinone ring, which cannot be epimerized at a later stage of the synthesis.

2.2. Catalytic 1,3-dipolar cycloaddition of nitrones to unsaturated lactones

The insufficient *exo*/*endo* selectivity of the reactions investigated, which limits their practical application in target-oriented synthesis, prompted us to focus our attention on the catalytic variant of the investigated reactions.

Beginning in the early 1980s, Lewis acid-catalyzed 1,3-dipolar cycloadditions started to play an important role in this field of research.[17,19] The efficiency of the catalysts relies not only on their capability to enhance the reaction rate and yield but also on their ability to affect the stereochemical course of the process by influencing the reaction regiochemistry, as well as its *exo*/*endo*-, diastereo-, and enantioselectivity.

Compounds, such as $MgBr_2{\cdot}Et_2O$, ZnI_2, and titanium-based Lewis acids such as $TiCl_4$ and $Ti(O\textit{i}\text{-}Pr)_2Cl_2$ have been explored as potential catalysts for 1,3-dipolar cycloadditions. In pioneering works, Kanemasa et al. showed that certain Lewis acids such as $ZnCl_2$ and $Ti(O\textit{i}\text{-}Pr)_2Cl_2$ can catalyze 1,3-dipolar cycloadditions that result in *endo*-derived isoxazolidines with respect to the substituted olefin, while metal catalysts such as $MgBr_2{\cdot}Et_2O$ and $ZnBr_2$, promote the formation of *exo*-derived isoxazolidines.[20] Tamura et al. further extended this line of research by using $MgBr_2{\cdot}Et_2O$ as a Lewis acid catalyst in cycloaddition reactions with a chiral nitrone and allylic alcohols.[21] A few other groups have also reported that $BF_3{\cdot}Et_2O$ can be used as an efficient promoter for Lewis acid-assisted stereocontrolled cycloadditions with nitrones.[22] In 1997, Kobayashi et al.[23] reported the $Yb(OTf)_3$ catalyzed reactions of diarylnitrones with electron-poor olefins. They reported that the reaction yield strongly depended on the solvent; non-polar solvents such as hexane, benzene, or toluene were the most appropriate to provide the *endo* cycloadducts predominantly. The same preference was also observed by Jørgensen et al.[24] A year later, Komatsu et al.[25] demonstrated that for the same reaction the change of solvent from toluene to MeCN allowed to control the diasteroselectivity of the reaction to be controlled.

Based on these reports, we started to test the influence of Lewis acid additives on the stereochemical outcome of the investigated reactions. Initial screening of various Lewis acids, for instance MgI_2, $MgBr_2{\cdot}Et_2O$, $Zn(OTf)_2$, $Cu(OTf)_2$, $InCl_3$, $In(OTf)_3$, $FeCl_3$, and $Yb(OTf)_3$, revealed that only the ytterbium salt provided promising results. Following the Kobayashi protocol,[23] in the presence of a ytterbium salt, the corresponding cycloadducts were obtained with poor yield (<10%) but with high stereoselectivity providing almost exclusively the *exo* isomers. Better results were obtained when $Sc(OTf)_3$ was used instead of $Yb(OTf)_3$. The best results for $Sc(OTf)_3$ were observed when the reaction was performed in toluene at room temperature. The replacement of toluene with CH_2Cl_2 led to a decrease in the yield, but the stereoselectivity remained at the same level. In the case of MeCN, as reported by Komatsu et al.[25] the formation of a product was not observed.

With preliminary studies in hand, we directed our attention to the unsubstituted lactones **11** and **14**, and protected lactones **10**, **13**, and **15** (Table 1). Since a catalytic reaction could not be performed if the lactone had a free hydroxyl group (we did not observe formation of any product), the cycloaddition to lactone **12** was not investigated further. The influence of the catalyst was demonstrated by the cycloaddition of **10** and nitrone **21**. Under the thermal conditions a mixture of adducts **29** and **30** was formed in 54% yield and with a ratio of approximately 77:23, respectively. In the presence of the catalyst, the ratio of adducts was 96:4, respectively, and the yield was 60%. It should be noted that this cycloaddition reaction was found to be reversible. Heating of the kinetic product **29** caused its isomerization to **30** in 21% after 24 h. Further extension of reflux time in toluene increased the amount of isomer **30** to 41% after 72 h, and 49% after 96 h (Fig. 1). This observation demonstrated the reversibility of the cycloaddition and the preference of the phenyl substituent at C3 to occupy the convex-side of the bicyclic skeleton.

The catalytic effect of $Sc(OTf)_3$ was also demonstrated for other reactions (Table 1). Benzyl protected lactone **15** gave a mixture of **31** and **32**; under thermal conditions, adducts were formed in 43% yield in a ratio of 67:33, whereas in the presence of the catalyst, the yield was 51% and the ratio was 96:4, respectively. The same results were obtained when nitrone **9**, obtained from anisaldehyde, was used. Under the thermal conditions, a mixture of **33** and **34** was obtained in a 41% yield and a ratio of approximately 63:37, respectively, whereas in the presence of the catalyst a mixture of the same adducts, in a ratio of 96:4, was obtained in 51% yield.

Under thermal conditions, unsubstituted lactone **14** yielded a mixture of **35** and **36** in 56% yield and in a ratio of 73:27, whereas in the presence of a catalyst on adducts, a mixture was formed in 60% yield and a ratio of 96:4, respectively. Heating the kinetic product **35** showed the following: after 3 days 22% of **36**, after 10 days 42% of **36**, and after 38 days 62% of **36**. Due to the instability of nitrones, a further extension of the heating resulted in a decrease of the reaction yield.

Five-membered lactones **11** and **13** reacted under thermal conditions with diphenyl nitrone **21** to give mixtures of *exo* and *endo* adducts **37**/**38** and **39**/**40** with similar yields and ratios of the products. Under the thermal conditions compounds **37** and **38** were obtained in 56% yield and in a ratio of approximately 6:4, whereas **39** and **40** were obtained in 60% yield and a ratio of 73:27, respectively. In the presence of the acid catalyst, *exo* adducts **37** and **39** dominated in a ratio: 96:4 and 98:2, respectively, however, the reaction yield was significantly lower (29–33%). Recently, we have shown that the 5-substituted γ-lactones underwent racemization via a hydroxyl-furan tautomer.[10b] It could be postulated that the hydroxyl-furan tautomer of **11** and **13** is also responsible for the lower stability of the substrate in the presence of an acid catalyst.

Analogous reactions performed with lactones **13** and **15** using *N*-benzyl-nitrone **20** resulted in the formation, in each case, of mostly the kinetic *exo* products **41** and **43**, respectively, under both thermal and catalytic conditions, but in a much lower yield compared to that recorded for diphenyl nitrone **21**.

Table 1
Thermal and $Sc(OTf)_3$-catalyzed reaction of nitrones **9**, **20**, and **21** with sugar-derived lactones

Entry	Nitrone	Lactone	Products	Thermal conditions[a]		Catalytic conditions[b]	
				Yield (%)	*dr*	Yield (%)	*dr*
1	**21**	**10**	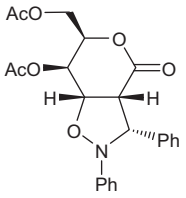 **29** 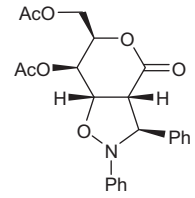 **30**	54	77:23	60	96:4
2	**21**	**15**	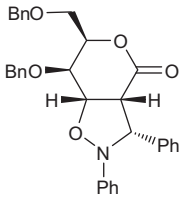 **33** 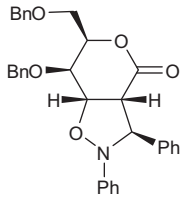 **34**	43	67:33	51	96:4
3	**9**	**15**	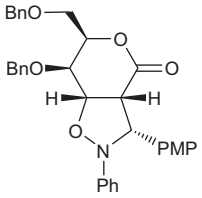 **33** 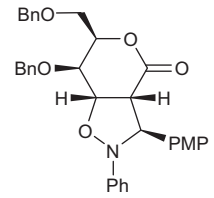 **34**	41	63:37	51	96:4
4	**21**	**14**	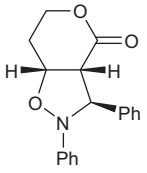 **35** 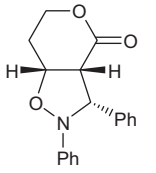 **36**	56	73:27	60	96:4
5	**21**	**11**	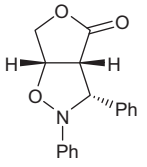 **37** 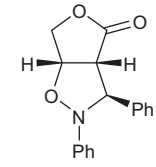 **38**	56	60:40	33	96:4
6	**21**	**13**	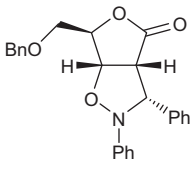 **39** 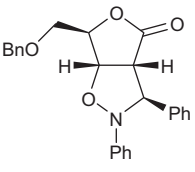 **40**	60	73:27	29	96:4
7	**20**	**13**	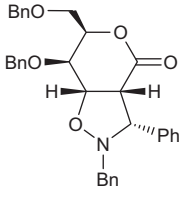 **43** 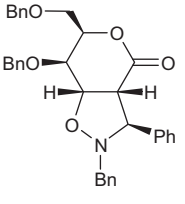 **44**	28	75:35	17	96:4

(*continued on next page*)

Table 1 (*continued*)

Entry	Nitrone	Lactone	Products	Thermal conditions[a]		Catalytic conditions[b]	
				Yield (%)	*dr*	Yield (%)	*dr*
8	**20**	**15**	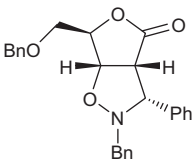 **41** 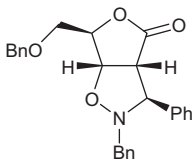 **42**	38	68:32	19	96:4

[a] Reaction conditions: nitrone (1.5 mmol), lactone (1 mmol) in PhMe at 115 °C.
[b] Reaction conditions: nitrone (1.5 mmol), lactone (1 mmol), $Sc(OTf)_3$ (0.1 mmol), MS 4 Å (400 mg) in PhMe at 30 °C; PMP: *p*-methoxyphenyl.

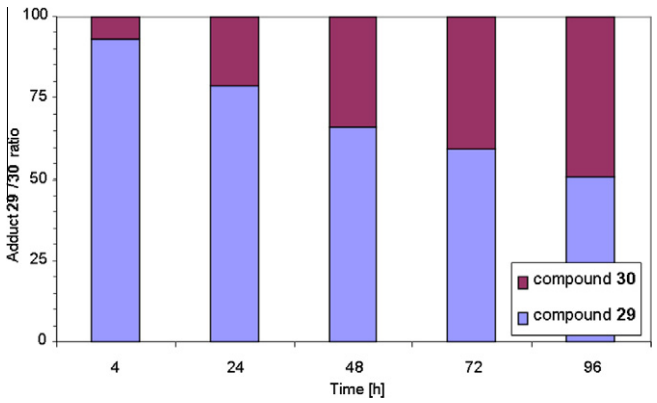

Figure 1. Change of the **29**/**30** ratio during elongated heating of adduct **29** obtained under kinetic control conditions (in the presence of $Sc(OTf)_3$). Isomerization was performed in boiling toluene.

2.3. Theoretical studies on thermal and LA-catalyzed 1,3-dipolar cycloadditions of diarylnitrones and unsaturated lactones

The enhancement of the reaction of nitrones **18**–**21** with sugar-derived unsaturated lactones **11**–**16** encouraged us to further study this process by the application of computational methods. There are several examples of computational studies on 1,3-DCA reactions involving nitrones[26] including studies on the Lewis acid effect.[27]

Recently, we have also investigated 1,3-dipolar cycloadditions of five-membered nitrone **17** with α,β-unsaturated γ- and δ-lactones **11** and **14** through molecular orbital calculations at the B3LYP/6-31+G(d) level theory to find a good agreement with the experimental data.[11] These successful studies prompted us to use similar calculations to characterize the 1,3-dipolar cycloadditions between lactones **11** and **14** and diphenyl nitrone **21** and compare them with experimental results in order to explain the stereochemical pathway involving substituted congeners **13** and **15**.

2.3.1. Computational methods

The initial geometry optimization and conformational search of reactants and products were carried out using the HyperChem v.7.51 suite of applications.[28] For all molecular modeling calculations the MM+ force field[29] was used. The final geometry optimization of the stationary points was carried out using DFT methods at the B3LYP[30] and MP3[31] level theory with 6-31+G(d,p) basis set implemented with GAUSSIAN 03 suite of software.[32] The optimizations were carried out using a Berny analytical gradient method[33] or QST3 method.[34] The stationary points were characterized by the frequency calculations in order to verify that the minima and transition structures (TSs) had zero and one imaginary frequency, respectively. The electronic structures of the stationary points and bond orders (Wiberg indexes)[35] were analyzed by the natural bond orbital method (NBO).[36] The intrinsic reaction coordinates (IRC)[37] were also calculated to analyze the mechanism in detail for all of the transition structures obtained. The solvent effect was treated by the single-point calculation for gas-phase stationary points using the self-consistent reaction field (SCRF)[38] based on the polarizable continuum model (PCM) reported by Tomasi et al.[39]

The electronic chemical potential μ[40] and chemical hardness η[41] values were approximated in terms of the one-electron energies of the frontier molecular orbitals HOMO and LUMO (E_{HOMO}, E_{LUMO}) using Eqs. (1) and (2), respectively:

$$\mu = \frac{\varepsilon_{HOMO} + \varepsilon_{LUMO}}{2} \quad (1)$$

$$\eta = \varepsilon_{LUMO} - \varepsilon_{HOMO} \quad (2)$$

$$\bar{\omega} = \frac{\mu^2}{2\eta} \quad (3)$$

$$S = \frac{1}{2\eta} \quad (4)$$

at the ground state of molecules. The global electrophilicity power ω was evaluated using Eq. (3) whereas global softness S is given by Eq. (4).[42]

2.3.2. Study on the thermal 1,3-DC between diphenylnitrone 21 and unsaturated valerolactone 14

As a computational model, we investigated the theoretical outcome of the reaction between *C*,*N*-diphenylnitrone **21** and six-membered lactone **14** (Scheme 3). For the sake of clarity, nitrone **21** is assigned as **N** and lactone **14** as **L**. As shown in Table 1, the reaction between these to reagents provides two bicyclic isoxazolidines **35** and **36** in a ratio of 73:27, under thermal conditions, or in a ratio of 96:4 in the presence of a scandium salt catalyst. For the sake of clarity, these compounds are marked as **P-1** and **P-2**, respectively.

For the model reaction, the two distinct regioisomeric approach modes of the oxygen atom of **N** relative to the β-conjugated position of lactone **L**, named *meta* and *ortho*, are possible. These two approaches led to regioisomeric isoxazolidines **P-1**/**P-2** and **P-1′**/**P-2′** (Scheme 3).

The 1,3-DCA reaction investigated has been analyzed using global reactivity indices defined in the context of conceptual DFT[43] which is a useful and powerful tool to understand the behavior of cycloadditions.[41,44] The frontier molecular orbital energies and the global properties are provided in Table 2.

The HOMO/LUMO energy gaps ($LUMO_2/HOMO_1$ 4.118 eV and $LUMO_1/HOMO_2$ 5.543 eV) between reactants **N** and **L** indicate that the $LUMO_2/HOMO_1$ interaction is predominant, which is typical for normal electron-demand cycloaddition reactions (Table 2, Fig. 2).

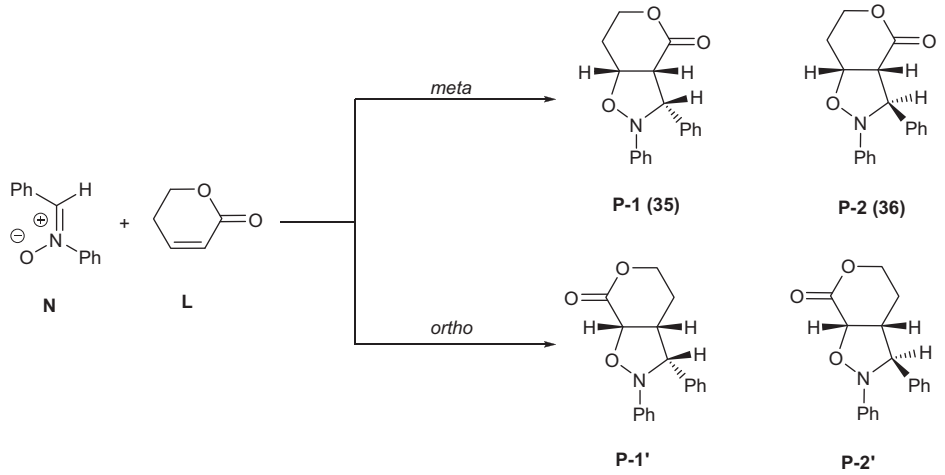

Scheme 3.

Table 2
DFT/6-31+G(d,p) calculated frontier orbital energies and static global reactivity indices

Molecule	E_{HOMO} (a.u.)	E_{LUMO} (a.u.)	μ (a.u.)	η (a.u.)	ω (eV)	S (a.u.)
N	−0.21554	−0.07525	−0.14540	0.14029	2.05	3.564046
Sc–N complex	−0.27270	−0.12266	−0.19768	0.15004	3.54	3.332445
L	−0.27904	−0.06413	−0.17159	0.21491	1.86	2.326555
Sc–L complex	−0.28279	−0.12905	−0.20592	0.15374	3.75	3.252244

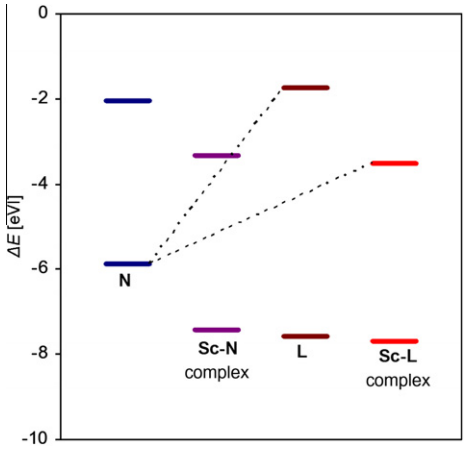

Figure 2. Energy diagram of HOMO and LUMO orbitals of nitrone **N**, lactone **L**, and their complexes with $ScCl_3$.

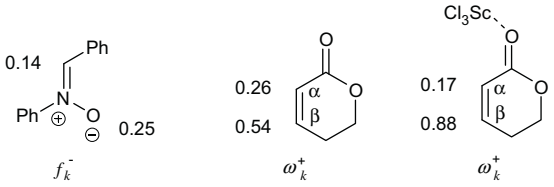

Figure 3. Nucleophilic Fukui function values (f_k^-) at nitrone **N** and the local electrophilicity values (ϖ_k^+) of free lactone **L** and its complex with $ScCl_3$.

The electronic chemical potential μ of nitrone **N** is higher than that calculated for lactone **L**, which indicates that the net charge transfer will take place from dipole **N** to dipolarophile **L**. This result is in agreement with the FMO energy predictions as well as the charge transfer analysis of TSs (vide infra). The electrophilicity powers of nitrone **N** and lactone **L** are 2.05 and 1.86 eV, respectively, which classify both of them as strong electrophiles. The low value of $\Delta\omega$ for the reaction of **N** and **L** (0.19 eV) indicates that the cycloaddition reaction will have a low polar character (vide infra).

An investigation of the local electrophilicity indices ϖ_k^+[45] at the electrophilic reagent and the nucleophilic Fukui functions f_k^-[46] at nucleophilic one can be useful for the prediction of the regioselectivity of a given reaction. Both calculated parameters, ϖ_k^+ for lactone **L** and f_k^- for nitrone **N**, respectively, are summarized in Figure 3.

The nitrone oxygen atom is a more reactive site for nucleophilic attack due to the larger value of f_k^- (0.25 eV) with respect to the nitrone carbon atom (0.14 eV). As one should expect, the C_β position of lactone **L** has a more electrophilic center of the molecule according to the analysis of local electrophilicity indices. Consequently, the preferred mode of nucleophilic attack of the nitrone **N** at the C_β position of lactone **L** should favor the formation type **P-1**/**P-2** regioisomers (*meta* channel); this was observed experimentally.

According to the above presented computational results and the experimental evidence, the formation of isoxazolidines **P-1′** and **P-2′** is omitted from further discussion and only the *exo*/*endo* selectivity of the reaction of **N** and **L** through a *meta* reactivity channel is considered.

As in our previous computational studies,[11] the search of stationary points was preceded by conformation analysis. The conformational search (in a range of 5 kcal/mol) using an MM+ force field led to identification of two conformers for **P-1** and two conformers for structure **P-2**, respectively. The re-calculation of the molecular geometries using DFT methods in the gas phase provided the optimized minimized geometries which are given in Figure 4. The relative energies for the conformers are also provided in Figure 4. As reported in Table 3, isoxazolidine **P-2** is thermodynamically more stable than adduct **P-1** by 1.2 kcal/mol.

An investigation of the potential energy surface (PES) made it possible to localize the stationary points for the *endo* and *exo* approach (Table 3, Fig. 5). Their analysis indicated a concerted mechanism for the cycloaddition in both cases.

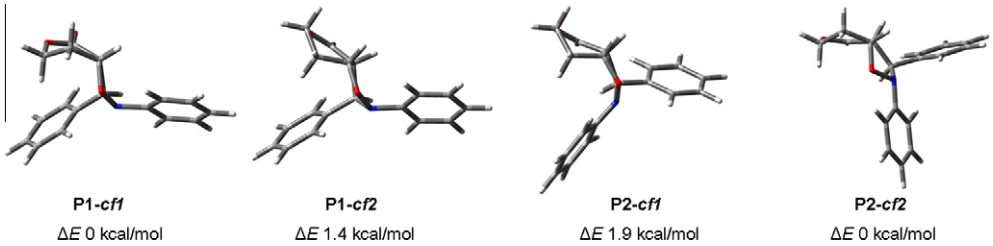

Figure 4. B3LYP/6-31+G(d,p) structures of conformational isomers of **P-1** and **P-2**. The relative energies are given in relation to the lowest energy conformer of *exo* and *endo*-adducts, respectively.

Table 3
Total/free (*E* and *G* in a.u.) and relative (Δ*E*, Δ*G* in kcal/mol) energies at 25 °C, for all stationary points of the reaction between nitrone **N** and lactone **L** in the gas phase and in toluene (DFT B3LYP/6-31+G(d,p))[a]

Geometry	Direct reaction in gas phase				Reverse rxn[b]		Direct reaction in toluene	
	E	Δ*E*	G	Δ*G*	Δ*E*	Δ*G*	*E*	Δ*E*
N	−631.7507702	—	−631.790127	—	—	—	−631.7510941	—
L	−344.4969027	—	−344.526469	—	—	—	−344.5026753	—
MC-1	−976.2523342	−2.9	−976.308699	5.0	27.5	27.2	−976.2613536	−4.8
TS-1[b]	−976.2173843	19.0	−976.264040	33.0			−976.2251513	18.0
P-1[b]	−976.2612332	−8.5	−976.307439	5.7			−976.2679945	−8.9
MC-2	−976.2545373	−4.3	−976.307758	5.5			−976.2615609	−4.9
TS-2[b]	−976.2126910	22.0	−976.260276	35.3	29.9	30.1	−976.2206596	20.8
P-2[b]	−976.2631089	−9.7	−976.310526	3.8			−976.2695633	−9.9

[a] All energies are referred to the energy of **N** + **L**; energies include ZPE correction.
[b] The lowest energy conformer.

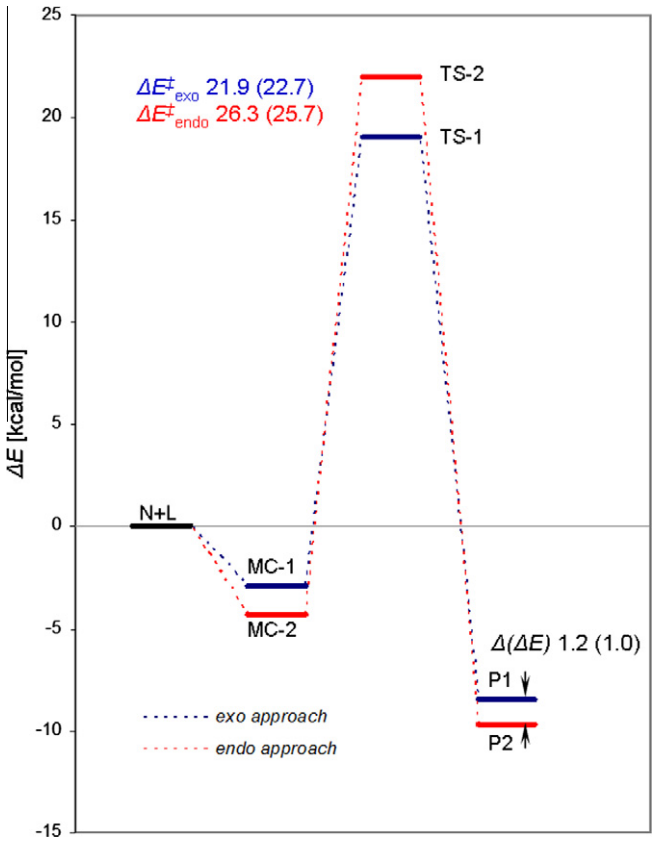

Figure 5. Energy profiles, in gas-phase and in toluene (in parenthesis) in kcal/mol, for the uncatalyzed 1,3-DC reaction between **N** and **L**.

For both reactive channels, two molecular complexes, **MC-1** and **MC-2**, respectively, associated with a very early step of the reaction, were found. **MC-1** and **MC-2** are located at 2.9 and 4.3 kcal/mol, respectively, below the reagents **N** and **L**.

The activation energies associated with the *exo* and *endo* approach of the reactants in the 1,3-DC reaction are 21.9 (**TS-1**) and 26.3 kcal/mol (**TS-2**), respectively. The formation of the cycloadducts **P-1** and **P-2** is exothermic by −8.5 and −9.7 kcal/mol, respectively.

The geometries, including conformers, of the TSs are given in Figure 6. The lengths of the forming O–C and C–C bonds for **TS-1** are 1.967 and 2.296 Å, respectively, and for **TS-2** 1.995 and 2.207 Å, respectively. These results confirm the concerted mechanism of the cycloaddition. However, due to the electron-deficient nature of the dipolarophile, the process is asynchronous in what can be seen, that is, the O···C distance is shorter than the C···C one. The same conclusion can be drawn when the bond order is taken into consideration. To follow the nature of the formation process for the C–O and C–C bonds, the Wiberg bond indexes were also computed using the NBO population analysis as implemented in GAUSSIAN 03 and the results are shown in Table 4. In both cases, the formation of the O–C bond is more advanced than the corresponding C–C bond, which also confirms the asynchronicity of the reaction. The lower energy *exo* transition state is slightly more advanced and more asynchronous than *endo* one.

The charge transfer (q_{CT}) values, taken from the natural population analysis (NPA),[34,36,47] are 0.02e for **TS-1**, and 0.01e for **TS-2**. These low values indicate that the TSs have a low polar character, which is in agreement with the low value of $\Delta\omega$ computed for this cycloaddition reaction. Moreover, the positive value of q_{CT} indicates the charge transfer from the nitrone to the lactone, which is also in clear agreement with the lower electronic potential μ of the lactone **L** compared to that of the nitrone **N** (see Table 1), and with the highly electrophilic character of the lactone.

Table 3 contains data of the single-point calculation of the gas-phase geometries using the PCM model. In toluene, all structures are stabilized in the range of 3–6 kcal/mol. The inclusion of a solvent decreased the energy difference between the activation bar-

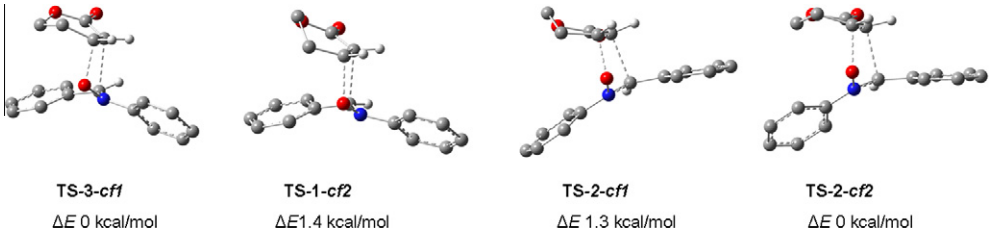

Figure 6. Transition states for reaction of the nitrone **N** with the lactone **L** (for clarity some hydrogen atoms are omitted).

Table 4
Distances for the forming bonds, Wiberg bond orders, and charge transfer (in terms of residual charge of the nitrone fragment in the transition state) for transition structures

Structure[a]	Atoms' distance (Å)		Bond order		NPA q_{CT} (e)
	O–C bond	C–C bond	O–C bond	C–C bond	
TS-1	1.967	2.296	0.42	0.33	0.02
TS-2	1.995	2.207	0.41	0.37	0.01

[a] The lowest energy conformer.

rier of the formation of **P-1** and **P-2** from 4.4 to 3.0 kcal/mol (Fig. 5), but the relationships within the energy profile presented in Figure 5 remained the same. This is due to the better solvation of **MC-1** compared to **MC-2** [this is in agreement with larger dipole moment of the former one (8.8 debye) than **MC-2** 2.6 debye].

The estimated high activation barrier of the *exo* and *endo* cycloadditions remains in agreement with the experimental evidence. As mentioned in a previous section, there was no formation of the desired product(s) when the reaction was carried out in toluene at room temperature (kinetic control conditions), thus, an increase of the temperature was required to perform the reaction between **N** and **L**. In this case the composition of the post-reaction mixture is influenced by the thermodynamic stability of the products. The comparison of the data from Table 3 indicates that under thermodynamic control, the **P-1**/**P-2** mixture in a ratio of ca. 7:1 should be expected (ΔE 1.2 kcal/mol) according to Boltzmann distribution analysis. A more accurate ratio is obtained when a solvent effect is included; in toluene, the estimated ratio is ca. 5:1 (ΔE 1.0 kcal/mol) which is close to the data presented in Table 1.

The differences between the calculated and experimental results may be caused by several factors. Although the elevated temperature is used to accelerate the cycloaddition, it is difficult to confirm that the reaction proceeds under real thermodynamic control conditions. As a result, the composition of the reaction mixture cannot be estimated directly based on the relative stability of products. Of course, a solution could be to repeat the experiment in a higher boiling solvent and compare the results. However, that is not the case. The problem is the reversibility of the cycloaddition reaction and the stability of the nitrone, which resulted in a dramatic decrease of the reaction yield.

The computation study for the model process indicates that the activation barrier for *retro*-processes is only 1.3 to 1.4-fold higher than those for the forward reactions. This means that when the reaction of **N** with lactone **L** is conducted in refluxing toluene, the *retro*-cycloaddition process cannot be neglected. This is even more possible in a higher boiling solvent. It should be noted that the decomposition of the **P-1** product should be easier than that of the *endo*-isomer **P-2** due to its lower thermal stability and lower activation barrier (compare ***retro*-TS-1** and ***retro*-TS-2**). As demonstrated earlier, the reversibility of the cycloaddition can be easily demonstrated by extended heating of the *exo* product; after a period of time, the *endo* isomer along with starting lactone can be detected in the crude reaction mixture.

Finally, the outcome of the reaction of **N** with lactone **L** can also be affected by the fact that nitrones have limited thermal stability (for instance they can undergo a deoxygenation process leading to the corresponding imines which are commonly observed in the post-reaction mixture). Such decomposition seriously perturbs the cycloaddition reaction and, as a consequence, together with other factors, hinders the predictability of the composition of the post-reaction mixture.

2.3.3. Study on the 1,3-DC between diphenylnitrone 21 and unsaturated valerolactone 14 catalyzed by a scandium salt

As demonstrated earlier, the addition of a catalytic amount of $Sc(OTf)_3$ enhanced the cycloaddition between nitrones **9**, **20**, and **21** and the sugar-derived lactones to provide almost exclusively the corresponding *exo* adducts. The most important fact is that the presence of a scandium salt makes it possible to carry out the investigated 1,3-DC reactions at room temperature.

These results encouraged us to broaden our analysis of the catalytic variant of the cycloaddition through quantum mechanics methods. To simplify the computational model, the reaction of nitrone **N** with lactone **L** in the presence of $ScCl_3$ instead of $Sc(OTf)_3$ was investigated.

The catalytic effect of the Lewis acid (LA) can be achieved by the coordination of the scandium salt either by the nitrone or the lactone. According to the visualization in Figure 1 and the numerical data in Table 1, the coordination of the nitrone by the LA decreases the energy of its HOMO orbital but, at the same time, increases the $HOMO_{nitrone}/LUMO_{lactone}$ gap (from 4.1 to 5.7 eV). On the other hand, the lactone activation decreases its LUMO energy value resulting in a smaller frontier orbital's gap (from 4.1 to 2.4 eV) and a predominance of such an interaction.

The coordination of the LA to the lactone **L** changes its electronic chemical potential μ (Table 1), but it is still lower than the value for the nitrone indicating that the direction of the net charge transfer through the reaction remains the same. The activation of the lactone by the LA increases the lactone electrophilicity from 1.86 to 3.75 eV for the corresponding complex. Moreover, the large $\Delta\omega$ value for nitrone **N** and lactone $ScCl_3$–**L** complex (1.7 eV) indicates the large polar character of the catalyzed 1,3-DC reaction, which is in the agreement with further CT analysis (vide infra). As presented in Figure 2, the coordination of $ScCl_3$ to lactone **L** increases the local electrophilicity at the β-carbon atom of the corresponding complex to ca. 0.88 eV.

The search for stationary points for the catalyzed reaction between nitrone **N** and lactone **L** was preceded by an investigation of the structure of the lactone **L**/$ScCl_3$ complex. The PES analysis of the lactone $ScCl_3$–**L** complex resulted in generation of the two structures presented in Figure 7. The **Sc-L-*cf2*** structure, with the Lewis acid coordinated in an *anti*-relationship to the ring oxygen atom, is the lowest energy conformer, although the energy difference is quite small. Additionally, further calculations also confirmed that the *anti*-location of the LA with respect to the ring oxygen atom is also more preferred for other stationary points. Consequently, the **Sc-L-*cf2*** conformation of lactone **L**/$ScCl_3$ complex **Sc**–**L** was taken into consideration throughout further studies.

Similar to the uncatalyzed process described in Section 2.1, the effect of the Lewis acid was studied only for one reactivity channel, that is, the *meta* channel. As before, both the *exo* and *endo* approaches of the 1,3-dipole to the dipolarophile were analyzed.

The analysis of the potential energy surface revealed that the LA has a different effect depending on the *exo* or *endo* approach. Whereas the *exo* approach has a stepwise mechanism, with two transition states and one intermediate, the alternative *endo* cycloaddition has mostly a concerted character with only one transition state.

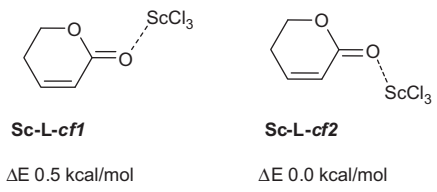

Figure 7. Two $ScCl_3$/lactone **L** complexes.

As for the non-catalyzed process, during the PES analysis for the scandium-catalyzed cycloaddition, two distinct molecular complexes **MC-3** and **MC-4**, were found (Table 5). **MC-3** and **MC-4** are located at 6.1–8.5 kcal/mol, respectively, below the reagents **N** and **Sc**–**L**. Along the *exo*-cycloaddition, the **TS-3-I** is located at 9.2 kcal/mol above **MC-3**. Highly confusing is the location of **IN**, which was found at 2 kcal/mol above the corresponding transition state **TS-3-I**. The second transition state **TS-3-II**, which corresponds to the C–C bond formation, is located at 1.2 kcal/mol above the intermediate. Along the *endo* approach, the **TS-4** is located at 16.7 kcal/mol above **MC-4**. The formation of cycloadducts **P-3** (adduct **P-1**/$ScCl_3$ complex) and **P-4** (adduct **P-2**/$ScCl_3$ complex) is exothermic by −12.9 and −11.4 kcal/mol, respectively (Table 5).

Initially, it was suspected that the deviation of energy values for polar species **IN**, as well as **TS-3-II**, resulted from the calculation that did not consider the presence of the solvent, that is in the gas phase. However, the single-point calculation involving the solvent effect did not resolve the problem (Table 5). The energy gap between **TS-3-I** and **IN** was smaller but the latter one (**IN**) was still higher in energy.

As reported previously for studies on Diels–Alder reactions, the HF calculations overestimate the activation barrier energy, whereas the MP2 calculations underestimate that energy.[48] Thus, during studies on the $AlCl_3$-catalyzed 1,3-DCA Domingo et al.[27c,47,49] reported that MP3 calculations are a more suitable method for providing reasonable activation energies. Therefore, the single-point calculations at MP3 level were carried out for all stationary points optimized by the DFT method. The comparison of the relative energies calculated at both levels can be found in Table 6.

Table 5
B3LYP/6-31+G(d,p) total (*E*, in a.u.) and relative[a] (*ΔE*, kcal/mol) energies, in gas phase, dichloromethane and toluene, of the stationary points involved in the *exo* and *endo* approaches of the 1,3-DCA of nitrone **N** and lactone **L** in the presence of $ScCl_3$

Geometry	In gas phase		In dichloromethane		In toluene	
	E	Δ*E*	*E*	Δ*E*	*E*	Δ*E*
Sc–L	−2486.181265	—	−2486.211260	—	−2486.197459	—
N	−631.9588851	—	−631.9677013	—	−631.9634539	—
MC-3	−3118.149802	−6.1	−3118.180386	−0.9	−3118.167216	−3.7
TS-3-I	−3118.135294	3.1	−3118.164657	9.0	−3118.150916	6.3
IN	−3118.132008	5.1	−3118.163671	9.6	−3118.148886	7.6
TS-3-II	−3118.130099	6.3	−3118.159213	12.3	−3118.145616	9.6
P-3	−3118.160658	−12.9	−3118.187831	−5.6	−3118.174727	−18.3
MC-4	−3118.153635	−8.5	−3118.181538	−1.6	−3118.168235	−4.6
TS-4	−3118.126987	8.3	−3118.153925	15.7	−3118.141197	12.4
p-4	−3118.158305	−11.4	−3118.186170	−4.5	−3118.172547	−7.3

[a] Relative to reactants, ZPE correction was not included.

Table 6
MP3/6-31+G(d,p) total (*E*, a.u.) and relative energies (Δ*E*, kcal/mol),[a] in gas phase and toluene and dichloromethane, of the stationary points involved in the *exo* approach of the 1,3-DCA of nitrone **N** and lactone **Sc**–**L** complex in the presence of $ScCl_3$

Geometry	MP3/6-31+G(d,p)					
	Gas phase		Toluene		Dichloromethane	
N	−630.0804285	—	−630.0853176	—	−630.0898512	—
Sc–L	−2482.614343	—	−2482.622384	—	−2482.638102	—
MC-3	−3112.716699	−13.8	−3112.732754	−15.7	−3112.747861	−12.5
TS-3-I	−3112.700048	−3.3	−3112.717370	−6.1	−3112.732855	−3.1
IN	−3112.707531	−8.0	−3112.726368	−11.7	−3112.743026	−9.5
TS-3-II	−3112.698003	−2.0	−3112.715418	−4.8	−3112.730834	−1.8
P-3	−3112.750014	−34.7	−3112.765908	−36.5	−3112.780983	−33.3
MC-4	−3112.715851	−13.2	−3112.732105	−15.3	−3112.747246	−12.1
TS-4	−3112.694891	−0.1	−3112.712741	−3.2	−3112.727152	0.5
P-4	−3112.747251	−32.9	−3112.763409	−35.0	−3112.779104	−32.1

[a] Relative to reactants, ZPE correction was not included.

The MP3 calculations predict the higher stabilization of **MC-3** and **MC-4** with respect to B3LYP ones. The same trend is observed for the energies of products coordinated to $ScCl_3$ (**P-3** and **P-4**) (Table 6, Fig. 8). Although the MP3 calculations give higher stabilization of **MC-3**, the first activation barrier of the stepwise *exo* cycloadditions calculated at both theory levels is similar and equals 9.2 kcal/mol (B3LYP) and 10.5 kcal/mol, respectively. A large divergence was found for the relative energies of **IN** and **TS-3-II**, which may result from the overestimation of the energy of the highly polar **IN** species by B3LYP calculations. Now, the intermediate **IN** is located at 4.7 kcal/mol below the transition state **TS-3-I**, as one should expect. As a result, the activation energy of the second step, that is, C–C bond formation, increases from 1.2 (B3LYP) to 6.0 kcal/mol.

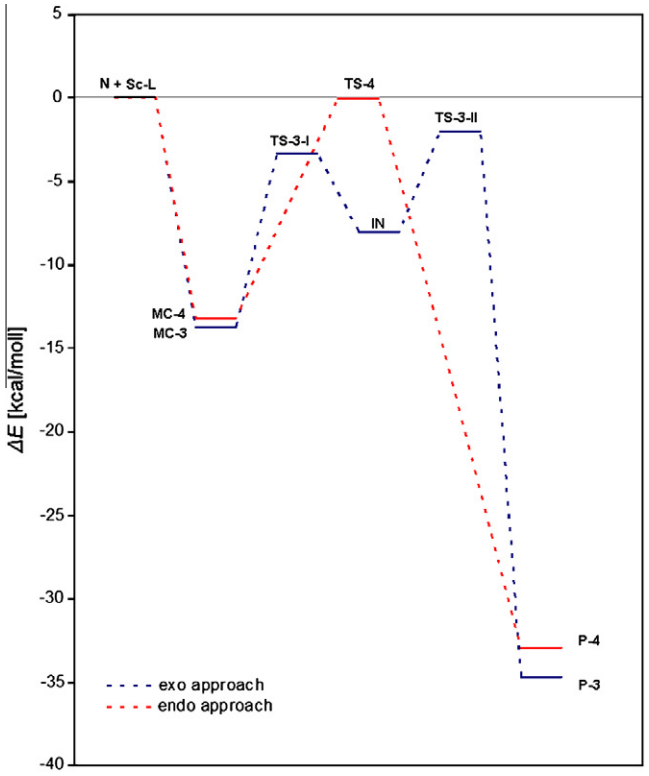

Figure 8. Energy profile [MP3/6-31+(d,p)], in gas-phase, for the $ScCl_3$-catalyzed 1,3-DC reactions between nitrone **N** and lactone **L**.

Analogous to the concerted process leading to the *endo* adduct **P-4**, the MP3 calculated activation barrier is lower by 3.5 kcal/mol than the value obtained with B3LYP. However, the MP3 method still gives the correct *exo*/*endo* selectivity with the *exo* approach being the preferred process over the *endo* one. The activation energy difference is 2.8 kcal/mol.

The geometries of the transition states and the intermediate involved in the two aforementioned stereochemical approaches are shown in Figure 9 and the numerical data associated with bond lengths and orders are given in Table 7. In the case of the *exo* approach, the first step is the nucleophilic attack of the oxygen atom of **N** at the β-position of the **Sc–L** complex, which proceeds through the **TS-3-I** transition state. The length of the forming O···C bond is 1.860 Å, while the distance between the corresponding carbon

Table 7
Distances for the forming bonds, Wiberg bond orders, and charge transfer (in terms of residual charge of the nitrone fragment in the stationary points) for the transition structures and the intermediate in Lewis acid catalyzed cycloaddition of nitrone **N** to the **Sc–L** complex

Structure	Atoms' distance (Å)		Bond order		NPA q_{CT} (e)
	O–C bond	C–C bond	O–C bond	C–C bond	
TS-3-I	1.860	3.387	0.40	0.03	0.28
IN	1.581	3.142	0.67	0.03	0.49
TS-3-II	1.564	2.535	0.64	0.20	0.26
TS-4	1.909	2.338	0.51	0.29	0.21

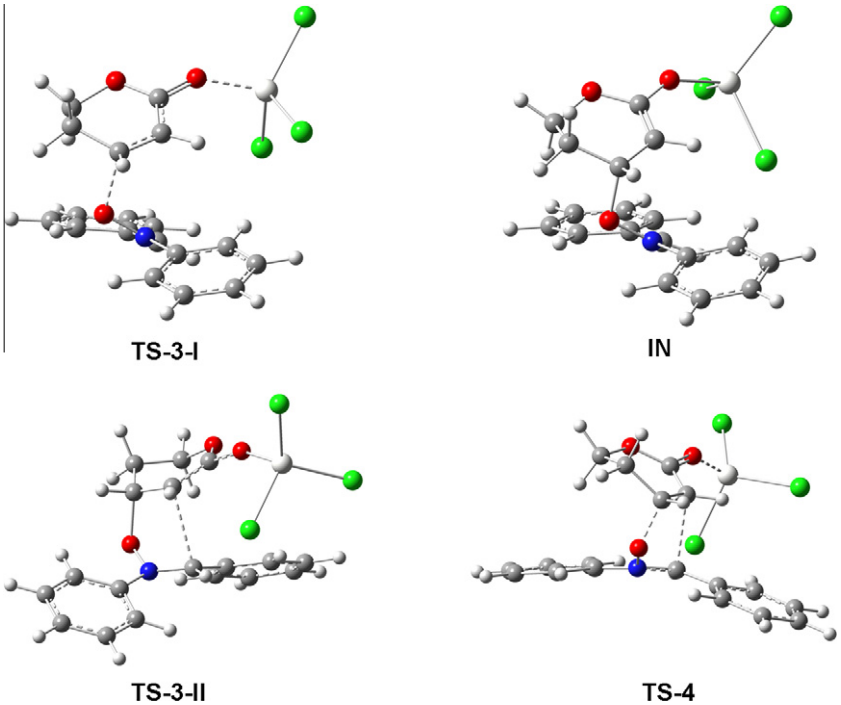

Figure 9. Structures of the TSs and the intermediate involved in the $ScCl_3$-catalyzed 1,3-DC reactions between nitrone **N** and lactone **L**.

atoms at nitrone and lactone becomes 3.387 Å. The O···C bond order for **TS-3-I** is 0.40, whereas for C···C it is only 0.03. The O–C bond length of the corresponding intermediate **IN** is 1.581 Å while the C/C distance remains 3.142 Å. The O–C bond order for **IN** is 0.67. In the transition state associated with C–C bond formation **TS-3-II**, the distance of both carbon atoms comes to 2.535 Å and the bond order is 0.2. The O···C and C···C distances at **TS-4**, leading to the *endo* adduct **P-4**, are 1.909 and 2.338 Å, respectively. The bond orders are 0.51 and 0.29. Such a large difference between the length and order of both forming bonds indicates the asynchronicity of the cycloaddition.

The values of the charge transfer (CT) along with *exo* and *endo* cycloaddition are reported in Table 7. In the LA-catalyzed reaction of nitrone **N** to the **Sc–L** complex, the charge flows from the 1,3-dipole to the dipolarophilic species for both stereochemical approaches. The CT of the nucleophilic attack of **N** to the **Sc–L** complex along the stepwise process is: 0.13e at **MC-3** and 0.28e at **TS-3-I**. In the *endo* process, CT values are 0.12e at **MC-4** and 0.21e for **TS-4**. The large CT values obtained for **MC-3** and **MC-4** indicate the large electronic interaction between both reactants and justify the large stabilization energy during the formation of these molecular complexes. At the stepwise process going from **TS-3-I** to **IN**, the CT values increase from 0.28e to 0.49e, which indicates the highly Zwitterionic character of these species. The large polar character of the investigated cycloaddition with respect to the non-catalyzed process is in full agreement with the large increase of the electrophilicity of lactone **L** as a result of coordination with the LA. Consequently, such coordination leads to an increase of $\Delta\omega$ for the catalyzed cycloaddition after which it becomes a more polar process.

Bearing in mind the large polar character of the transition states and the intermediate involved in the Lewis acid catalyzed 1,3-DCA reaction, it should be expected that the solvent effect has a large influence on the energies. The results of the single-point calculations of the gas-phase geometries (MP3 method) using PCM model are presented in Table 6. In toluene as well as in dichloromethane, the solvent effects stabilize all the species in the range of 5–22 kcal/mol. With the inclusion of the solvent effect, the **TS-3-I** activation barrier is equal to 9.7 (toluene) and 9.4 kcal/mol (dichloromethane). Due to the Zwitterionic character of **IN**, it can be stabilized by a solvent, which results in an increase of the activation energy barrier for **TS-3-II** (from 6.0 to 6.9 kcal/mol, in toluene, and to 7.7 kcal/mol in more polar dichloromethane). Nevertheless, the first step is still the rate-determining step. The MP3/PCM calculations provide somewhat confusing data for the activation energy barrier for the formation of *endo* adduct **P-4** (**TS-4** $\Delta E^{\ddagger}$ 13.2 kcal/mol in gas-phase vs 12.2 and 12.6 kcal/mol for toluene and dichloromethane, respectively). An expected trend can be found for the data obtained by B3LYP/PCM calculations; now, after inclusion of the solvent, the activation energy changes from 16.7 up to 17.3 kcal/mol due to the slightly larger solvent stabilization of the molecular complex than the transition state.

Solvent effect calculations confirm that the coordination of Lewis acid to the dipolarophile significantly accelerates the cycloaddition reaction by a strong reduction of the activation energies. These calculations also confirm that the higher acceleration of the formation of the *exo* adduct compared to the *endo* adduct is what makes the scandium salt catalyzed 1,3-dipolar cycloaddition highly diastereoselective.

3. Conclusions

We have reported the $Sc(OTf)_3$-catalyzed 1,3-dipolar cycloaddition reactions between acyclic nitrones and six-membered sugar-derived lactones. Under the catalytic variant, the cycloadditions proceed under mild conditions at room temperature to provide almost exclusively *exo* adducts with high stereoselectivity.

The mechanism of the 1,3-dipolar cycloaddition of *C*,*N*-diphenylnitrone with unsaturated valerolactone under thermal and Lewis acid-mediated conditions has been studied using DFT and MP3 methods. Computational results indicated that in the absence of a Lewis acid, the reaction takes place through an asynchronous concerted mechanism with a low polar character and provides the *exo* cycloadduct as a major product in full agreement with the experimentally observed trends.

The coordination of a scandium salt to the lactonic dipolarophile results in significant changes of the cycloaddition reaction investigated, resulting in a large enhancement of the electrophilicity of the $ScCl_3$/lactone complex. However, the addition of a Lewis acid has a different effect on the reaction mechanism depending on the trajectory of the approach of the reactant. As demonstrated, in the formation of the *exo* product, the reaction mechanism is changed from concerted into stepwise proceeding through an Zwitterionic intermediate. The intermediate is formed by nucleophilic attack of the nitrone oxygen atom at the highly electrophilic β-conjugated position of the Sc/lactone complex. This Michael-type addition is the rate-determining step. The product is formed through subsequent intramolecular ring closure. In the *endo* approach, the reaction mechanism is mostly concerted, although it appears to be highly asynchronous. The computed activation energy barriers confirm the high diastereoselectivity observed experimentally.

As demonstrated, the influence of Lewis acid on the outcome of the cycloaddition reaction investigated, particularly its regioselectivity, can also be correctly explained by analysis of the global and local reactivity indices.

4. Experimental

4.1. General

^1H and ^{13}C NMR spectra were recorded on a Varian VN MRS Spectrometer at 600 and 150 MHz, respectively, in $CDCl_3$ or C_7D_8. TMS was used as the internal standard. Chemical shifts are reported as δ values in ppm, and coupling constants are in Hertz. The proton assignment was carried out based on COSY experiments. Infrared spectra were recorded on a FT-IR-1600 Perkin–Elmer spectrophotometer. CD spectra were recorded on a Jasco J-815 spectropolarimeter. Optical rotations were recorded on a Jasco P-2000 polarimeter. High-resolution mass spectra were recorded on an ESI-TOF Mariner Spectrometer (Perspective Biosystem) or a Synapt G2-S Waters Spectrometer for electrospray ionization. Thin layer chromatography was performed on Merck aluminum sheet Silica Gel 60 F254. Column chromatography was carried out using Merck silica gel (230–400 mesh). Diastereoisomers' ratios of the reactions investigated were assigned by ^1H NMR or/and HPLC analysis.

Nitrones **9** and **20**–**21**[50] and unsaturated lactones **10**, **13**, **15**, and **16**[16] were obtained following the literature procedures. Lactones **12** and **14** were purchased from Aldrich. Lactone **11** was obtained from furfural according to the literature procedure.[51]

4.2. Thermal 1,3-dipolar cycloaddition—general procedure

Lactone (1 mmol) and nitrone (1.5 mmol) were dissolved in toluene (10 ml) and refluxed for 24 h, after which the solvent was removed under reduced pressure and the residue was chromatographed on silica gel.

4.3. Catalytic 1,3-dipolar cycloaddition—general procedure

The mixture of $Sc(OTf)_3$ (0.1 mmol) and MS 4 Å (400 mg) in dry PhMe (10 ml) was stirred for 30 min at room temperature. Next, the lactone (1 mmol) and nitrone (1.5 mmol) were added and reaction mixture was kept at 30 °C for 72 h, after which the molecular sieves were filtered off and residue was chromatographed on silica gel.

4.4. (3*R*,3a*R*,6*R*,7*S*,7a*S*)-7-(Acetoxy)-6-(acetoxymethyl)-2,3-diphenyltetrahydro-2*H*-pyrano[3,4-*d*]isoxazol-4(6*H*)-one 29

Oil; $[\alpha]_D^{20} = -57$ (*c* 1.2, $CHCl_3$); ^1H NMR (600 MHz, $CDCl_3$, signals for Ph hydrogen atoms are omitted) δ: 5.45 (1H, d, *J* 9.0 Hz), 5.27 (1H, dd, *J* 1.9, 1.4 Hz), 4.59 (1H, dd, *J* 4.8, 2.1 Hz), 4.40–4.38 (1H, m), 4.11 (1H, dd, *J* 11.6, 5.4 Hz), 3.96 (1H, t, *J* 9.1 Hz), 3.90 (1H, dd, *J* 11.7, 10.4 Hz), 2.07 (3H, s), 1.98 (3H, s); ^{13}C NMR (150 MHz, $CDCl_3$, signal of Ph carbon atoms are omitted) δ: 170.1, 169.4, 166.2, 75.8, 73.8, 73.6, 71.4, 65.4, 61.5, 52,2, 20.6; HRMS (ESI) *m*/*z* calcd for $[M+Na]^+$ $C_{23}H_{23}NO_7Na$ 448.1366; found 448.1388; IR (film) *v*: 1747 cm^{-1}.

4.5. (3*S*,3a*R*,6*R*,7*S*,7a*S*)-7-(Acetoxy)-6-(acetoxymethyl)-2,3-diphenyltetrahydro-2*H*-pyrano[3,4-*d*]isoxazol-4(6*H*)-one 30

Oil; $[\alpha]_D^{20} = +76$ (*c* 1.3, $CHCl_3$); ^1H NMR (600 MHz, $CDCl_3$, signals for Ph hydrogen atoms are omitted) δ: 5.40 (1H, dd, *J* 3.1, 1.5 Hz), 5.10–5.08 (1H, m), 4.71 (1H, dd, *J* 7.5, 3.1 Hz), 4.59 (1H, d, *J* 2.1 Hz), 4.29 (1H, dd, *J* 11.8, 5.6 Hz), 4.24 (1H, dd, *J* 11.8, 7.0 Hz), 3.65 (1H, dd, *J* 7.4, 6,1 Hz), 2.11 (3H, s), 2.09 (3H, s); ^{13}C NMR (150 MHz, $CDCl_3$) δ: 170.3, 169.3, 167.8, 73.8, 73.2, 73.1, 71.4, 64.2, 61.9, 54.9, 20,7; HRMS (ESI) *m*/*z* calcd for $[M+Na]^+$ $C_{23}H_{23}NO_7$-Na 448.1366; found 448.1388; found; IR (film) *v*: 1747 cm^{-1}.

4.6. (3*R*,3a*R*,6*R*,7*S*,7a*S*)-7-(Benzyloxy)-6-(benzyloxymethyl)-2,3-diphenyltetrahydro-2*H*-pyrano[3,4-*d*]isoxazol-4(6*H*)-one 31

Oil; $[\alpha]_D^{20} = -62.4$ (*c* 1.12, $CHCl_3$); ^1H NMR (600 MHz, C_7D_8, signals for Ph hydrogen atoms are omitted) δ: 5.15 (1H, d, *J* 8.7 Hz), 4.66 (1H, dd, *J* 9.4, 4.4 Hz), 4.43 (1H, d, *J* 12.0 Hz), 4.32 (1H, d, *J* 12.0 Hz), 4.16–4.13 (1H, m), 4.02 (1H, d, *J* 11.4 Hz), 3.95 (1H, d, *J* 11.4 Hz), 3.86 (1H, dd, *J* 4.3, 3.2 Hz), 3.67 (1H, t, *J* 9.1 Hz), 3.37 (1H, dd, *J* 9.6, 3.6 Hz), 3.33 (1H, dd, *J* 10.2, 6.6 Hz); ^{13}C NMR (150 MHz, C_7D_8, signals for Ph carbon atoms are omitted) δ: 165.9, 76.4, 75.3, 72.8, 72.3, 71.7, 70.6, 66.9, 52.6; HRMS (ESI) *m*/*z* calcd for $[M+Na]^+$ 544.2099; found 544.2105; IR (film) *v*: 1741 cm^{-1}.

4.7. (3*S*,3a*R*,6*R*,7*S*,7a*S*)-7-(Benzyloxy)-6-(benzyloxymethyl)-2,3-diphenyltetrahydro-2*H*-pyrano[3,4-*d*]isoxazol-4(6*H*)-one 32

Oil; $[\alpha]_D^{20} = +46.1$ (*c* 1.1, $CHCl_3$); ^1H NMR (600 MHz, C_7D_8, signals for Ph carbon atoms are omitted) δ: 4.77 (1H, dd, *J* 8.3, 4.7 Hz), 4.64 (1H, d, *J* 6.2, Hz), 4.56–4.53 (1H, m), 4.47 (1H, d, *J* 11.9 Hz) 4.28 (1H, d, *J* 11.9 Hz), 4.10 (1H, d, *J* 11.8 Hz), 4.09 (1H, d, *J* 11.8 Hz), 3.88–3.86 (1H, m), 3.73 (1H, dd, *J* 8.3, 6.2 Hz), 3.58 (1H, dd, *J* 9.9, 4.2 Hz), 3.49 (1H, dd, *J* 9.9, 5.7 Hz); ^{13}C NMR (150 MHz, C_7D_8, signals for Ph carbon atoms are omitted) δ: 168.0, 75.7, 75.5, 73.2, 72.3, 72.2, 71.7, 67.5, 54.1; HRMS (ESI) *m*/*z* calcd for $[M+Na]^+$ 544.2099; found 544.2102; IR (film) *v*: 1742 cm^{-1}.

4.8. (3*R*,3a*R*,6*R*,7*S*,7a*S*)-7-(Benzyloxy)-6-(benzyloxymethyl)-3-(4-methoxyphenyl)-2-phenyltetrahydro-2*H*-pyrano[3,4-*d*]isoxazol-4(6*H*)-one 33

Oil; $[\alpha]_D^{20} = -69$ (*c* 1.1, $CHCl_3$); ^1H NMR (600 MHz, C_7D_8, signals for Ph hydrogen atoms are omitted) δ: 5.12 (1H, d, *J* 8.6 Hz), 4.66 (1H, dd, *J* 9.4, 4.4 Hz), 4.46 (1H, d, *J* 12.0 Hz), 4.34 (1H, d, *J* 12.0 Hz), 4.24–4.18 (1H, m), 4.05 (1H, d, *J* 11.8 Hz), 3.96 (1H, d, *J* 11.8 Hz), 3.87 (1H, dd, *J* 4.1, 3.1 Hz), 3.66 (1H, t, *J* 9.0 Hz), 3.40 (1H, dd, *J* 9.6, 3.7 Hz), 3.35 (1H, dd, *J* 9.8, 6.2 Hz); ^{13}C NMR (150 MHz, C_7D_8, signals for Ph carbon atoms are omitted) δ: 165.8, 76.5, 75.7, 72.4, 72.1, 71.6, 70.7, 66.9, 54.2, 52.6; IR (film) *v*: 1747 cm^{-1}; HRMS (ESI) *m*/*z* calcd for $C_{34}H_{33}NO_6Na$ $[M+Na]^+$ 574.2206; found 574.2202.

4.9. (3*S*,3a*R*,6*R*,7*S*,7a*S*)-7-(Benzyloxy)-6-(benzyloxymethyl)-3-(4-methoxyphenyl)-2-phenyltetrahydro-2*H*-pyrano[3,4-*d*]isoxazol-4(6*H*)-one 34

$[\alpha]_D^{20} = +27$ (*c* 1, $CHCl_3$); ^1H NMR (600 MHz, C_7D_8, signals for Ph hydrogen atoms are omitted) δ: 4.79 (1H, dd, *J* 8.2, 4.6 Hz), 4.63 (1H, d, *J* 6.0 Hz), 4.56–4.52 (1H, m), 4.47 (1H, d, *J* 11.9 Hz) 4.28 (1H, d, *J* 11.9 Hz), 4.10 (1H, d, *J* 11.8 Hz), 4.09 (1H, d, *J* 11.8 Hz), 3.88–3.85 (1H, m), 3.74 (1H, dd, *J* 8.2, 6.1 Hz), 3.57 (1H, dd, *J* 9.8, 4.2 Hz), 3.47 (1H, dd, *J* 9.7, 5.6 Hz), 3.26 (3H, s); ^{13}C NMR (150 MHz, C_7D_8) δ: 168.0, 75.7, 75.4, 73.1, 72.2, 72.4, 71.6, 67.6, 56.2, 54.2; IR (film) *v*: 1747 cm^{-1}; HRMS (ESI) *m*/*z* calcd for $C_{34}H_{33}NO_6Na$ $[M+Na]^+$ 574.2206; found 574.2204.

4.10. (3*R**,3a*R**,7a*R**)-2,3-Diphenyltetrahydro-2*H*-pyrano[3,4-*d*]isoxazol-4(6*H*)-one 35

Oil; ^1H NMR (600 MHz, $CDCl_3$, signals for Ph hydrogen atoms are omitted) δ: 5.49 (1H, d, *J* 9.3 Hz), 4.76 (1H, dt, *J* 9.2, 3.1 Hz), 3.97 (2H, dd, *J* 7.2, 3.8 Hz), 3.90 (1H, t, *J* 9.0 Hz), 2.08–2.04 (2H, m); ^{13}C NMR (150 MHz, $CDCl_3$) δ: 167.9, 149.2, 137.0, 129.3, 128.5, 128.1, 127.5, 122.8, 114.4, 73.5, 71.2, 64.3, 53.4; 26.3; IR (film) *v*: 1743 cm^{-1}; HRMS (EI) *m*/*z* calcd for $C_{18}H17NO_3$ [M] 295.1208; found 295.1205.

4.11. (3*S**,3a*R**,7a*R**)-2,3-Diphenyltetrahydro-2*H*-pyrano[3,4-*d*]isoxazol-4(6*H*)-one 36

Oil; ^1H NMR (600 MHz, C_7H_8, signals for Ph hydrogen atoms are omitted) δ: 4.75 (d, *J* 3.0 Hz, 1H), 4.14 (dd, *J* 6.2, 4.7 Hz, 1H), 3.94 (d, *J* 10.9 Hz, 1H), 3.46 (dd, *J* 10.9, 4.6 Hz, 1H), 2.54 (dd, *J* 6.4, 3.1 Hz, 1H); IR (film) *v*: 1743 cm^{-1}; HRMS (EI) *m*/*z* calcd for $C_{18}H_{17}NO_3$ [M] 295.1208; found 295.1205.

4.12. (3*R**,3a*R**,6a*S**)-2,3-Diphenyltetrahydrofuro[3,4-*d*]isoxazol-4(2*H*)-one 37

Oil; ^1H NMR (600 MHz, C_7D_8, signals for Ph hydrogen atoms are omitted) δ: 4.43 (1H, d, *J* 9.0 Hz), 4.25–4.23 (1H, ddd, *J* 8.1, 6.5, 2.9 Hz), 4.00 (1H, dd, *J* 10.3, 2.9 Hz), 3.62 (1H, dd, *J* 10.2, 6.5 Hz), 2.88 (1H, dd, *J* 9.0, 8.1 Hz); ^{13}C NMR (150 MHz, C_7D_8, signals for Ph carbon atoms are omitted) δ:171.4, 77.3, 72.1, 70.3, 53.8; IR (film) *v*: 1741 cm^{-1}; HRMS (EI) *m*/*z* calcd for $C_{17}H_{15}NO_3$ [M] 281.1052; found 281.1050.

4.13. (3*S**,3a*R**,6a*S**)-2,3-Diphenyltetrahydrofuro[3,4-*d*]isoxazol-4(2*H*)-one 38

Oil; ^1H NMR (600 MHz, C_7D_8) δ: 4.76 (1H, d, *J* 3.0 Hz), 4.15 (1H, dd, *J* 6.4, 4.5 Hz), 3.94 (1H, d, *J* 10.9 Hz), 3.46 (1H, dd, *J* 10.9, 4.5 Hz), 2.54 (1H, dd, *J* 6.4, 3.0 Hz); ^{13}C NMR (150 MHz, C_7D_8, signals for Ph carbon atoms are omitted) δ: 174.7, 77.7, 71.6, 69.8, 56.9; IR (film) *v*: 1742 cm^{-1}; HRMS (EI) *m*/*z* calcd for $C_{17}H_{15}NO3$ [M] 281.1052; found 281.1049.

4.14. (3*R*,3a*R*,6*R*,6a*S*)-6-(Benzyloxymethyl)-2,3-diphenyltetrahydrofuro[3,4-*d*]isoxazol-4(2*H*)-one 39

Oil; $[\alpha]_D^{20} = -61$ (*c* 1.1, $CHCl_3$); ^1H NMR (600 MHz, C_7D_8, signals for Ph hydrogen atoms are omitted) δ: 4.76 (1H, dd, *J* 7.5, 2.1 Hz), 4.47 (1H, d, *J* 9.0 Hz), 4.41 (1H, dd, *J* 4.9, 2.5 Hz), 4.15 (1H, d, *J*, 12.0 Hz), 4.08 (1H, d, *J*, 12.0 Hz), 3.30 (1H, dd, *J* 9.0, 7.5 Hz), 3.19 (1H, dd, *J* 10.7, 3.0 Hz), 3.10 (dd, *J* 10.7, 2.6 Hz); ^{13}C NMR (150 MHz, C_7D_8, signals for Ph carbon atoms are omitted) δ: 171.2, 81.1, 79.9, 73.3, 72.2, 69.5, 55.4 HRMS (EI) *m*/*z* calcd for $C_{25}H_{24}NO_4$ [M] 402.1705; found 402.1701; IR (film) *v*: 1781 cm^{-1}.

4.15. (3*S*,3a*R*,6*R*,6a*S*)-6-(Benzyloxymethyl)-2,3-diphenyltetrahydrofuro[3,4-*d*]isoxazol-4(2*H*)-one 40

Oil; $[\alpha]_D^{20} = +94$ (*c* 1.1, $CHCl_3$); ^1H NMR (600 MHz, C_7D_8, signals for Ph hydrogen atoms are omitted) δ: 4.90 (1H, d, *J* 3.1 Hz), 4.68 (1H, d, *J* 6.4 Hz), 4.30 (1H, t, *J* 2.5 Hz), 4.02 (1H, d, *J* 12.2 Hz), 3.97 (1H, d, *J* 12.2 Hz), 3.48 (1H, dd, *J* 6.4, 3.2 Hz), 3.11 (1H, dd, *J* 10.6, 3.0 Hz), 3.10 (dd, *J* 10.6, 2.3 Hz); ^{13}C NMR (150 MHz, C_7D_8, signals for Ph carbon atoms are omitted) δ: 174.9, 80.9, 79.5, 73.1, 71.7, 69.0, 58.6 HRMS (EI) *m*/*z* calcd for $C_{25}H_{24}NO_4$ [M] 402.1705; found 402.1700; IR (film) *v*: 1777 cm^{-1}.

4.16. (3*R*,3a*R*,6*R*,6a*S*)-*N*-Benzyl-6-(benzyloxymethyl)-3-phenyltetrahydrofuro[3,4-*d*]isoxazol-4(2*H*)-one 41

Oil; $[\alpha]_D^{20} = -59$ (*c* 1.0, $CHCl_3$); ^1H NMR (600 MHz, C_7D_8, signals for Ph hydrogen atoms are omitted) δ: 4.57 (1H, dd, *J* 7.9, 2.0 Hz), 4.34 (1H, d, *J* 2.4 Hz), 4.12 (1H, dd, *J* 12.0 Hz), 4.02 (1H, dd, *J* 12.0 Hz), 3.85 (1H, d, *J* 14.4 Hz), 3.55 (1H, d, *J* 8.0 Hz), 3.36 (1H, d, *J* 14.4 Hz), 3.13 (1H, dd, *J* 10.7, 2.5 Hz), 3.04 (1H, t, *J* 7.9 Hz), 2.95 (1H, dd, *J* 10.7, 2.5 Hz); ^{13}C NMR (150 MHz, C_7D_8, signals for Ph carbon atoms are omitted) δ: 171.8, 83.6, 78.2, 73.2, 73.1, 69.7, 59.0, 54.1; HRMS (EI) *m*/*z* calcd for $C_{26}H_{26}NO_4$ [M] 416.1862; found 416.1856; IR (film) *v*: 1775 cm^{-1}.

4.17. (3*S*,3a*R*,6*R*,6a*S*)-*N*-Benzyl-6-(benzyloxymethyl)-3-phenyltetrahydrofuro[3,4-*d*]isoxazol-4(2*H*)-one 42

Oil; $[\alpha]_D^{20} = +78$ (*c* 1.0, $CHCl_3$); ^1H NMR (600 MHz, C_7D_8, signals of Ph hydrogen atoms are omitted) δ: 4.52 (1H, d, *J* 6.2 Hz), 4.14 (1H, br s), 4.06 (1H, d, *J* 12.2 Hz), 4.04–3.98 (1H, m), 3.97 (1H, d, *J* 12.2 Hz), 3.78–3.65 (1H, m), 3.54 (1H, d, *J* 14.3 Hz), 3.42 (1H, dt), 3.06 (1H, d, *J* 9.2 Hz), 2.81 (1H, d, *J* 9.2 Hz); ^{13}C NMR (150 MHz, C_7D_8, signals for Ph carbon atoms omitted) δ: 175.5, 80.4, 79.9, 74.0, 73.2, 69.3, 59.3 58.2; HRMS (EI) *m*/*z* calcd for $C_{26}H_{26}NO_4$ [M] 416.1862; found 416.1859; IR (film) *v*: 1778 cm^{-1}.

4.18. (3*R*,3a*R*,6*R*,7*S*,7a*S*)-2-Benzyl-7-(benzyloxy)-6-(benzyloxymethyl)-3-phenyltetrahydro-2*H*-pyrano[3,4-*d*]isoxazol-4(6*H*)-one 43

Oil; $[\alpha]_D^{20} = -61$ (*c* 1.1, $CHCl_3$); ^1H NMR (600 MHz, C_7D_8, signals for Ph hydrogen atoms are omitted) δ: 4.96 (1H, br s), 4.35 (1H, dd, *J* 5.8, 3.8 Hz), 4.26 (1H, d, *J* 12.0 Hz), 4.15 (2H, m), 4.07 (1H, d, *J* 12.0 Hz), 3.85 (1H, d, *J* 8.7 Hz), 3.80–3.74 (2H, m), 3.59 (1H, t, *J* 8.7 Hz), 3.54 (1H, dd, *J* 9.5, 4.6 Hz), 3.51–3.43 (2H, m); ^{13}C NMR (150 MHz, C_7D_8, signals for Ph carbon atoms are omitted) δ: 166.0, 75.8, 75.0, 72.9, 72.8, 72.7, 72.3, 67.6, 59.5, 53.1; HRMS (ESI) *m*/*z* calcd for $C_{34}H_{33}NO_5Na$ $[M+Na]^+$ 558.2256; found 558.2266; IR (film) *v*: 1742 cm^{-1}.

4.19. (3*S*,3a*R*,6*R*,7*S*,7a*S*)-2-Benzyl-7-(benzyloxy)-6-(benzyloxymethyl)-3-phenyltetrahydro-2*H*-pyrano[3,4-*d*]isoxazol-4(6*H*)-one 44

Oil; $[\alpha]_D^{20} = +117.5$ (*c* 1.3, $CHCl_3$); ^1H NMR (600 MHz, C_7D_8, signals for Ph hydrogen atoms are omitted) δ: 4.35 (1H, br s), 4.16 (1H, br s), 3.98 (1H, d, *J* 11.9 Hz), 3.93 (1H, d, *J* 12.3 Hz), 3.81 (1H, d, *J* 12.3 Hz), 3.79 (1H, d, *J* 12.5 Hz), 3.49 (1H, br s), 3.40 (1H, br s), 3.21 (2H, m), 3.25 (1H, br s), 3.21–3.17 (1H, m), 3.12 (1H, d, *J* 14.5 Hz); ^{13}C NMR (150 MHz, C_7D_8, signals for Ph carbon atoms are omitted) δ: 167.3, 75.6, 74.8, 74.3, 73.2, 71.8, 71.4, 67.9, 55.2; HRMS (EI) *m*/*z* calcd for $C_{34}H_{33}NO_5$ [M] 536.2437; found 536.2441; IR (film) *v*: 1741, cm^{-1}.

Acknowledgment

Authors are grateful to the European Union within European Regional Development Fund (Project POIG.01.01.02.-14-102/09) for financial support of research.

References

1. Veinberg, G.; Vorona, M.; Shestakova, I.; Kanepe, I.; Lukevics, E. *Curr. Med. Chem.* **2003**, *10*, 1744–1758.
2. (a) Tufariello, J. J. *Acc. Chem. Res.* **1979**, *12*, 396–403; (b) Tufariello, J. J.; Tette, J. P. *J. Org. Chem.* **1975**, *40*, 3866–3869.
3. (a) Denmark, S. E.; Cottell, J. J. *J. Org. Chem.* **2001**, *66*, 4276–4284; (b) Denmark, S. E.; Hurd, A. R. *J. Org. Chem.* **2000**, *65*, 2875–2886; (c) Denmark, S. E.; Thorarensen, A. *J. Am. Chem. Soc.* **1997**, *119*, 125–137; (d) DeShong, P.; Dicken, C. M.; Leginus, J. M.; Whittle, R. R. *J. Am. Chem. Soc.* **1984**, *106*, 5598–5602; (e) DeShong, P.; Leginus, J. M. *J. Am. Chem. Soc.* **1983**, *105*, 1686–1688; (f) Funk, R. L.; Bolton, G. L.; Daggett, J. U.; Hansen, M. M.; Horcher, L. H. M. *Tetrahedron* **1985**, *41*, 3479–3495; (g) Goti, A.; Cardona, F.; Brandi, A. *Synlett* **1996**, 761–763; (h) Goti, A.; Cicchi, S.; Cacciarini, M.; Cardona, F.; Fedi, V.; Brandi, A. *Eur. J. Org. Chem.* **2000**, 3633–3645; (i) Goti, A.; Cicchi, S.; Fedi, V.; Nannelli, L.; Brandi, A. *J. Org. Chem.* **1997**, *62*, 3119–3125; (j) Goti, A.; Fedi, V.; Nannelli, L.; De Sarlo, F.; Brandi, A. *Synlett* **1997**, 577–579; (k) Holmes, A. B.; Bourdin, B.; Collins, I.; Davison, E. C.; Rudge, A. J.; Stork, T. C.; Warner, J. *Pure Appl. Chem.* **1997**, *69*, 531–536; (l) Kliegel, W. *Pharmazie* **1977**, *32*, 411–416; (m) McCaig, A. E.; Meldrum, K. P.; Wightman, R. H. *Tetrahedron* **1998**, *54*, 9429–9446; (n) Schwartz, M. A.; Swanson, G. C. *J. Org. Chem.* **1979**, *44*, 953–958; (o) Tufariello, J. J.; Meckler, H.; Senaratne, K. P. A. *Tetrahedron* **1985**, *41*, 3447–3453.
4. (a) Bays, H. E.; Moore, P. B.; Drehobl, M. A.; Rosenblatt, S.; Toth, P. D.; Dujovne, C. A.; Knopp, R. H.; Lipka, L. J.; LeBeaut, A. P.; Yang, B.; Mellars, L. E.; Cuffie-Jackson, C.; Veltri, E. P. *Clin. Ther.* **2001**, *23*, 1209–1230; (b) Burnett, D. A.; Caplen, M. A.; Davis, H. R.; Burrier, R. E.; Clader, J. W. *J. Med. Chem.* **1994**, *37*, 1733–1736; (c) Chen, L.-Y.; Zaks, A.; Chackalamannil, S.; Dugar, S. *J. Org. Chem.* **1996**, *61*, 8341–8343; (d) Clader, J. W. *J. Med. Chem.* **2003**, *47*, 1–9; (e) Dugar, S.; Clader, J. W.; Chan, T.-M.; Davis, H. *J. Med. Chem.* **1995**, *38*, 4875–4877; (f) Ghosal, A.; Zbaida, S.; Chowdhury, S. K.; Iannucci, R. M.; Feng, W.; Alton, K. B.; Patrick, J. E.; Davis, H. R. Pat. Appl. **2002**.; (g) Knopp, R. H.; Gitter, H.; Truitt, T.; Bays, H.; Manion, C. V.; Lipka, L. J.; LeBeaut, A. P.; Suresh, R.; Yang, B.; Veltri, E. P. *Eur. Heart J.* **2003**, *24*, 729–741.
5. Keri, R. S.; Hosamani, K. M.; Reddy, H. S.; Shingalapur, R. V. *Arch. Pharm.* **2010**, *343*, 237–247.
6. Aslanian, R. G.; Bennett, C. E.; Burnett, D. A.; Chan, T. -Y.; Kiselgof, E. Y.; Knutson, C. E.; Harris, J. M.; McKittrick, B. A.; Palani, A.; Smith, E. M.; Vaccaro, H. M.; Xiao, D.; Kim, H. M., Pat. Appl. WO 2008/033464A2, **2008**.
7. (a) Banik, I.; Becker, F. F.; Banik, B. K. *J. Med. Chem.* **2002**, *46*, 12–15; (b) Meegan, M. J.; Carr, M.; Knox, A. J. S.; Zisterer, D. M.; Lloyd, D. G. *J. Enzyme Inhib. Med. Chem.* **2008**, *23*, 668–685.
8. (a) Panfil, I.; Chmielewski, M. *Tetrahedron* **1985**, *41*, 4713–4716; (b) Panfil, I.; Chmielewski, M.; Bełżecki, C. *Heterocycles* **1986**, *24*, 1609–1617; (c) Panfil, I.; Bełżecki, C.; Chmielewski, M. *J. Carbohydr. Chem.* **1987**, *6*, 463–470; (d) Panfil, I.; Bełżecki, C.; Urbanczyk-Lipkowska, Z.; Chmielewski, M. *Tetrahedron* **1991**, *47*, 10087–10094.
9. (a) Socha, D.; Jurczak, M.; Chmielewski, M. *Carbohydr. Res.* **2001**, *336*, 315–318; (b) Panfil, I.; Solecka, J.; Chmielewski, M. *J. Carbohydr. Chem.* **2006**, *25*, 673–684; (c) Paśniczek, K.; Socha, D.; Jurczak, M.; Solecka, J.; Chmielewski, M. *Can. J. Chem.* **2006**, *84*, 534–539; (d) Socha, D.; Paśniczek, K.; Jurczak, M.; Solecka, J.; Chmielewski, M. *Carbohydr. Res.* **2006**, *341*, 2005–2011; (e) Stecko, S.; Jurczak, M.; Urbańczyk-Lipkowska, Z.; Solecka, J.; Chmielewski, M. *Carbohydr. Res.* **2008**, *343*, 2215–2220; (f) Stecko, S.; Jurczak, M.; Staszewska-Krajewska, O.; Solecka, J.; Chmielewski, M. *Tetrahedron* **2009**, *65*, 7056–7063; (g) Stecko, S.; Paśniczek, K.; Jurczak, M.; Solecka, J.; Chmielewski, M. *Pol. J. Chem.* **2009**, *83*, 237–243; (h) Stecko, S.; Solecka, J.; Chmielewski, M. *Carbohydr. Res.* **2009**, *344*, 167–176.

10. (a) Stecko, S.; Paśniczek, K.; Jurczak, M.; Urbańczyk-Lipkowska, Z.; Chmielewski, M. *Tetrahedron: Asymmetry* **2006**, *17*, 68–78; (b) Stecko, S.; Paśniczek, K.; Jurczak, M.; Urbańczyk-Lipkowska, Z.; Chmielewski, M. *Tetrahedron: Asymmetry* **2007**, *18*, 1085–1093.
11. (a) Stecko, S.; Paśniczek, K.; Michel, C.; Milet, A.; Perez, S.; Chmielewski, M. *Tetrahedron: Asymmetry* **2008**, *19*, 2140–2148; (b) Stecko, S.; Paśniczek, K.; Michel, C.; Milet, A.; Pérez, S.; Chmielewski, M. *Tetrahedron: Asymmetry* **2008**, *19*, 1660–1669.
12. Stecko, S.; Frelek, J.; Chmielewski, M. *Tetrahedron: Asymmetry* **2009**, *20*, 1778–1790.
13. Michalak, M.; Stodulski, M.; Stecko, S.; Mames, A.; Panfil, I.; Soluch, M.; Furman, B.; Chmielewski, M. *J. Org. Chem.* **2011**, *76*, 6931–6936.
14. Michalak, M.; Stodulski, M.; Stecko, S.; Woźnica, M.; Staszewska-Krajewska, O.; Kalicki, P.; Furman, B.; Frelek, J.; Chmielewski, M. *Tetrahedron* **2012**, *68*, 10806–10817.
15. Stecko, S.; Michalak, M.; Stodulski, M.; Mucha, Ł.; Parda, K.; Furman, B.; Chmielewski, M. *Synthesis* **2012**, *44*, 2695–2698.
16. (a) Descotes, G.; Martin, J.-C. *Carbohydr. Res.* **1977**, *56*, 168–172; (b) Qiu, D.; Schmidt, R. R. *Synthesis* **1990**, 875–877; (c) Fazio, F.; Schneider, M. P. *Tetrahedron: Asymmetry* **2000**, *11*, 1869–1876; (d) Takhi, M.; Abdel-Rahman, A. A. H.; Schmidt, R. R. *Synlett* **2001**, 427–429.
17. Grigor'ev, I. A. *Nitrile Oxides, Nitrones, and Nitronates in Organic Synthesis*; John Wiley & Sons, Inc., 2007. pp 129–434.
18. Panfil, I.; Urbańczyk-Lipkowska, Z.; Chmielewski, M. *Pol. J. Chem.* **2005**, *79*, 239–249.
19. (a) Gothelf, K. V.; Jørgensen, K. A. *Chem. Rev.* **1998**, *98*, 863–910; (b) Gothelf, K. V.; Jorgensen, K. A. *Chem. Commun.* **2000**, 1449–1458; (c) Kanemasa, S. *Synlett* **2002**, 1371–1387; (d) Pellissier, H. *Tetrahedron* **2007**, *63*, 3235–3285; (e) Stanley, L. M.; Sibi, M. P. *Chem. Rev.* **2008**, *108*, 2887–2902.
20. (a) Kanemasa, S.; Uemura, T.; Wada, E. *Tetrahedron Lett.* **1992**, *33*, 7889–7892; (b) Kanemasa, S.; Tsuruoka, T.; Wada, E. *Tetrahedron Lett.* **1993**, *34*, 87–90; (c) Kanemasa, S.; Tsuruoka, T. *Chem. Lett.* **1995**, *24*, 49–50.
21. Tamura, O.; Shiro, T.; Ogasawara, M.; Toyao, A.; Ishibashi, H. *J. Org. Chem.* **2005**, *70*, 4569–4577.
22. (a) Frank, É.; Wölfling, J.; Aukszi, B.; König, V.; Schneider, T. R.; Schneider, G. *Tetrahedron* **2002**, *58*, 6843–6849; (b) Li, X.; Takahashi, H.; Ohtake, H.; Ikegami, S. *Heterocycles* **2003**, *59*, 547–571.
23. Kobayashi, S.; Akiyama, R.; Kawamura, M.; Ishitani, H. *Chem. Lett.* **1997**, 1039–1040.
24. Sanchez-Blanco, A. I.; Gothelf, K. V.; Jørgensen, K. A. *Tetrahedron Lett.* **1997**, *38*, 7923–7926.
25. Minakata, S.; Ezoe, T.; Nakamura, K.; Ryu, I.; Komatsu, M. *Tetrahedron Lett.* **1998**, *39*, 5205–5208.
26. (a) Sustmann, R.; Sicking, W.; Huisgen, R. *J. Am. Chem. Soc.* **1995**, *117*, 9679–9685; (b) Liu, J.; Niwayama, S.; You, Y.; Houk, K. N. *J. Org. Chem.* **1998**, *63*, 1064–1073; (c) Cossío, F. P.; Morao, I.; Jiao, H.; Schleyer, P. v. R. *J. Am. Chem. Soc.* **1999**, *121*, 6737–6746; (d) Carda, M.; Portolés, R.; Murga, J.; Uriel, S.; Marco, J. A.; Domingo, L. R.; Zaragozá, R. J.; Röper, H. *J. Org. Chem.* **2000**, *65*, 7000–7009; (e) Di Valentin, C.; Freccero, M.; Gandolfi, R.; Rastelli, A. *J. Org. Chem.* **2000**, *65*, 6112–6120; (f) Herrera, R.; Nagarajan, A.; Morales, M. A.; Méndez, F.; Jiménez-Vázquez, H. A.; Zepeda, L. G.; Tamariz, J. *J. Org. Chem.* **2001**, *66*, 1252–1263; (g) Kavitha, K.; Venuvanalingam, P. *J. Chem. Soc., Perkin Trans. 2* **2002**, 2130–2139; (h) Merino, P.; Mates, J. A.; Revuelta, J.; Tejero, T.; Chiacchio, U.; Romeo, G.; Iannazzo, D.; Romeo, R. *Tetrahedron: Asymmetry* **2002**, *13*, 173–190; (i) Merino, P.; Revuelta, J.; Tejero, T.; Chiacchio, U.; Rescifina, A.; Romeo, G. *Tetrahedron* **2003**, *59*, 3581–3592; (j) Aurell, M. J.; Domingo, L. R.; Pérez, P.; Contreras, R. *Tetrahedron* **2004**, *60*, 11503–11509; (k) Ess, D. H.; Houk, K. N. *J. Phys. Chem. A* **2005**, *109*, 9542–9553; (l) Grimme, S.; Mück-Lichtenfeld, C.; Würthwein, E.-U.; Ehlers, A. W.; Goumans, T. P. M.; Lammertsma, K. *J. Phys. Chem. A* **2006**, *110*, 2583–2586; (m) Merino, P.; Tejero, T.; Chiacchio, U.; Romeo, G.; Rescifina, A. *Tetrahedron* **2007**, *63*, 1448–1458; (n) Acharjee, N.; Banerji, A. *Comput. Theory Chem.* **2011**, *967*, 50–58.
27. (a) Domingo; Luis, R. *Eur. J. Org. Chem.* **2000**, 2265–2272; (b) Tanaka, J.; Kanemasa, S. *Tetrahedron* **2001**, *57*, 899–905; (c) Domingo, L. R.; Benchouk, W.; Mekelleche, S. M. *Tetrahedron* **2007**, *63*, 4464–4471.
28. HyperChem™ Professional 7.51, H., Inc., 1115 NW 4th Street, Gainesville, FL 32601, USA.
29. Hocquet, A.; Langgård, M. *J. Mol. Model.* **1998**, *4*, 94–112.
30. (a) Becke, A. D. *Phys. Rev. A* **1988**, *38*, 3098–3100; (b) Becke, A. D. *J. Chem. Phys.* **1993**, *98*, 5648–5652; (c) Lee, C.; Yang, W.; Parr, R. G. *Phys. Rev. B* **1988**, *37*, 785–789.
31. (a) Pople, J. A.; Binkley, J. S.; Seeger, R. *Int. J. Quantum Chem.* **1976**, *10*, 1–19; (b) Pople, J. A.; Seeger, R.; Krishnan, R. *Int. J. Quantum Chem.* **1977**, *11*, 149–163.
32. GAUSSIAN 09, Revision A.02; Frisch, M. J.; Trucks, G. W.; Schlegel, H. B.; Scuseria, G. E.; Robb, M. A.; Cheeseman, J. R.; Montgomery, J. A.; Vreven, T.; Kudin, K. N.; Burant, J. C.; Millam, J. M.; Iyengar, S. S.; Tomasi, J.; Barone, V.; Mennucci, B.; Cossi, M.; Scalmani, G.; Rega, N.; Petersson, G. A.; Nakatsuji, H.; Hada, M.; Ehara, M.; Toyota, K.; Fukuda, R.; Hasegawa, J.; Ishida, M.; Nakajima, T.; Honda, Y.; Kitao, O.; Nakai, H.H.; Klene, M.; Li, X.; Knox, J. E.; Hratchian, H. P.; Cross, J. B.; Adamo, C.; Jaramillo, J.; Gomperts, R.; Stratmann, R. E.; Yazyev, O.; Austin, A. J.; Cammi, R.; Pomelli, C.; Ochterski, J. W.; Ayala, P. Y.; Morokuma, K.; Voth, G. A.; Salvador, P.; Dannenberg, J. J.; Zakrzewski, V. G.; Dapprich, S.; Daniels, A. D.; Strain, M. C.; Farkas, O.; Malick, D. K.; Rabuck, A. D.; Raghavachari, K.; Foresman, J. B.; Ortiz, J. V.; Cui, Q.; Baboul, A. G.; Clifford, S.; Cioslowski, J.; Stefanov, B. B.; Liu, G.; Liashenko, A.; Piskorz, P.; Komaromi, I.; Martin, R. L.; Fox, D. J.; Keith, T.; Al-Laham, M. A.; Peng, C. Y.; Nanayakkara, A.; Challacombe, M.; Gill, P. M. W.; Johnson, B.; Chen, W.; Wong, M. W.; Gonzalez, C.; Pople, J. A.; GAUSSIAN, Inc.: Pittsburgh, PA, **2003**.
33. (a) Schlegel, H. B. *J. Comput. Chem.* **1982**, *3*, 214–220; (b) Schlegel, H. B. In *Modern Electronic Structure Theory*; Yarkony, D. R., Ed.; World Scientific: Singapore, 1994.
34. (a) Peng, C.; Schlegel, H. B. *Israel J. Chem.* **1993**, *33*, 449–454; (b) Peng, C.; Ayala, P. Y.; Schlegel, H. B.; Frisch, M. J. *J. Comput. Chem.* **1996**, *17*, 49–56.
35. Wiberg, K. B. *Tetrahedron* **1968**, *24*, 1083–1096.
36. Reed, A. E.; Weinstock, R. B.; Weinhold, F. *J. Chem. Phys.* **1985**, *83*, 735–746.
37. (a) Fukui, K. *Acc. Chem. Res.* **1981**, *14*, 363–368; (b) Head-Gordon, M.; Pople, J. A. *J. Chem. Phys.* **1988**, *89*, 5777–5786.
38. (a) Tomasi, J.; Persico, M. *Chem. Rev.* **1994**, *94*, 2027–2094; (b) Simkin, B. Y.; Sheikhet, I. *Quantum Chemical and Statistical Theory of Solutions—A Computational Approach*; Ellis Horwood: London, 1995.
39. (a) Cossi, M.; Barone, V.; Cammi, R.; Tomasi, J. *Chem. Phys. Lett.* **1996**, *255*, 327–335; (b) Cances, E.; Mennucci, B.; Tomasi, J. *J. Chem. Phys.* **1997**, *107*, 3032–3041; (c) Barone, V.; Cossi, M.; Tomasi, J. *J. Comput. Chem.* **1998**, *19*, 404–417.
40. (a) Parr, R. G.; Pearson, R. G. *J. Am. Chem. Soc.* **1983**, *105*, 7512–7516; (b) Parr, R. G.; Szentpály, L. v.; Liu, S. *J. Am. Chem. Soc.* **1999**, *121*, 1922–1924.
41. Domingo, L. R.; Aurell, M. J.; Pérez, P.; Contreras, R. *Tetrahedron* **2002**, *58*, 4417–4423.
42. Chattaraj, P. K.; Sarkar, U.; Roy, D. R. *Chem. Rev.* **2006**, *106*, 2065–2091.
43. (a) Geerlings, P.; De Proft, F.; Langenaeker, W. *Chem. Rev.* **2003**, *103*, 1793–1874; (b) Ess, D. H.; Jones, G. O.; Houk, K. N. *Adv. Synth. Catal.* **2006**, *348*, 2337–2361.
44. Pérez, P.; Domingo, L. R.; José Aurell, M.; Contreras, R. *Tetrahedron* **2003**, *59*, 3117–3125.
45. Domingo, L. R.; Aurell, M. J.; Pérez, P.; Contreras, R. *J. Phys. Chem. A* **2002**, *106*, 6871–6875.
46. Parr, R. G.; Yang, W. *J. Am. Chem. Soc.* **1984**, *106*, 4049–4050.
47. Reed, A. E.; Curtiss, L. A.; Weinhold, F. *Chem. Rev.* **1988**, *88*, 899–926.
48. (a) Bach, R. D.; McDouall, J. J. W.; Schlegel, H. B.; Wolber, G. J. *J. Org. Chem.* **1989**, *54*, 2931–2935; (b) Bachrach, S. M.; Liu, M. *J. Org. Chem.* **1992**, *57*, 6736–6744; (c) Li, Y.; Houk, K. N. *J. Am. Chem. Soc.* **1993**, *115*, 7478–7485; (d) Bachrach, S. M. *J. Org. Chem.* **1994**, *59*, 5027–5033.
49. Domingo, L. R.; Arnó, M.; Andrés, J. *J. Am. Chem. Soc.* **1998**, *120*, 1617–1618.
50. Brüning, I.; Grashey, R.; Hauck, H.; Huisgen, R.; Seidl, H. *Org. Synth.* **1966**, *46*, 127–130.
51. Näsman, J. H. *Org. Synth.* **1990**, *68*, 162–167.